

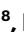
Induced pluripotent stem cell-derived cardiomyocyte in vitro models: benchmarking progress and ongoing challenges

Received: 11 December 2023

Accepted: 15 September 2024

Published online: 08 November 2024

 Check for updates

Jourdan K. Ewoldt ^{1,14}, Samuel J. DePalma ^{2,14}, Maggie E. Jewett ², M. Çağatay Karakan ^{1,3,4}, Yih-Mei Lin ⁵, Paria Mir Hashemian^{3,4}, Xining Gao^{1,6,7}, Lihua Lou ⁸, Micheal A. McLellan ^{1,7}, Jonathan Tabares ⁹, Marshall Ma^{3,4}, Adriana C. Salazar Coariti ¹⁰, Jin He ⁹, Kimani C. Toussaint Jr.^{10,11}, Thomas G. Bifano^{3,4}, Sharan Ramaswamy ⁵, Alice E. White ^{1,3,4,12,13}, Arvind Agarwal ⁸, Emma Lejeune³, Brendon M. Baker ²✉ & Christopher S. Chen ^{1,7}✉

Recent innovations in differentiating cardiomyocytes from human induced pluripotent stem cells (hiPSCs) have unlocked a viable path to creating in vitro cardiac models. Currently, hiPSC-derived cardiomyocytes (hiPSC-CMs) remain immature, leading many in the field to explore approaches to enhance cell and tissue maturation. Here, we systematically analyzed 300 studies using hiPSC-CM models to determine common fabrication, maturation and assessment techniques used to evaluate cardiomyocyte functionality and maturity and compiled the data into an open-access database. Based on this analysis, we present the diversity of, and current trends in, in vitro models and highlight the most common and promising practices for functional assessments. We further analyzed outputs spanning structural maturity, contractile function, electrophysiology and gene expression and note field-wide improvements over time. Finally, we discuss opportunities to collectively pursue the shared goal of hiPSC-CM model development, maturation and assessment that we believe are critical for engineering mature cardiac tissue.

The average cost to bring a new pharmaceutical to the market in the United States is estimated at more than 1 billion dollars¹, and approximately 10% of pharmaceuticals worldwide have been withdrawn due to adverse cardiovascular side effects². This high failure rate is in part due to the relative difficulty in predicting which drugs will have adverse cardiac effects. Primary human cardiomyocytes (CMs) are difficult to obtain and rapidly dedifferentiate in vitro, rendering them incapable of faithfully detecting anything but acute effects of pharmaceuticals on

the heart³. On the other hand, while animal models can reveal cardiotoxic and arrhythmogenic activity of pharmaceuticals, there are key differences in cardiac biology between species that limit their ability to fully predict the potential for adverse cardiovascular effects in humans⁴.

The advent of the first differentiation protocol of human embryonic stem cells (hESCs) into CMs in 1993 enabled researchers to study human CMs in vitro in ways not possible with primary CMs⁵. In 2007, the first hiPSCs were generated. Derived from skin or blood cells and

reprogrammed into a pluripotent state, these cells can be derived from patients and can be differentiated into CMs without the ethical challenges associated with sourcing hESCs⁶. Thus, this approach allows for the testing of pharmaceutical cardiovascular effects in a more physiologically relevant model⁷.

The use of hiPSC technology to generate human CMs has also enabled the study of myocardial physiology and pathobiology. Inherited cardiomyopathies, such as hypertrophic, dilated and arrhythmogenic cardiomyopathies (HCM, DCM, ACM), affect 1 in 500, 1 in 250 and 1 in 2,000–5,000 of the population, respectively⁸, and are caused by more than 1,000 possible genetic mutations across more than 100 genes^{9–11}. Patient-derived hiPSC-CM models of genetic cardiomyopathies and CRISPR–Cas9-edited hiPSC-CMs have thus been used to recapitulate disease in vitro, to shed light on new disease mechanisms and to establish gene-editing strategies to correct these diseases^{12–21}. Additionally, hiPSC-CMs have shown promise as regenerative therapies for patients with heart failure^{22,23}.

However, despite all the promise associated with hiPSC-CMs, the overall immaturity of hiPSC-CMs limits their utility. Fetal-like gene expression patterns, immature structure and function, and nonphysiologic or subphysiologic electromechanical activity are all important caveats to the conclusions drawn from studies using these cells to test pharmaceuticals or model disease states and are major hurdles for using these cells in regenerative or reparative therapies.

hiPSC-CMs typically exhibit immature structural phenotypes, including disorganized myofibrils, fewer mitochondria and poor colocalization of calcium channels and ryanodine receptors, which ultimately impair the functionality of hiPSC-CMs as compared to adult CMs (Table 1)²⁴. Additionally, engineered CMs mainly rely on glycolysis for energy, rather than more efficient energy production from oxidative phosphorylation used by adult CMs. Functionally, human adult CMs exhibit a resting membrane potential (RMP) and a conduction velocity of approximately –90 mV and 30–100 cm s⁻¹ (ref. 25), respectively, while very few hiPSC-CM models have shown an RMP below –80 mV (refs. 22,26–30) or a conduction velocity above 40 cm s⁻¹ (refs. 22,28,31). Additionally, the twitch force of adult human CMs is 25–44 mN mm⁻² (ref. 32), and only a few hiPSC-CM engineered constructs have achieved this level of contractility^{21,33}.

In the past decade, there have been great strides made toward understanding how to further mature hiPSC-CMs by combining knowledge from diverse fields. In achieving these advances, researchers have used many different cell lines, differentiation protocols, maturation techniques and functional assessments, making it challenging for the field to make head-to-head comparisons between studies. As the field of cardiac tissue engineering itself matures, standardized benchmarking across the field will be essential to extract key findings and apply them toward future advances.

To assess the current state of the art, we sought to systematically analyze a breadth of studies using hiPSC-CMs by extracting protocols and functional assessment metrics. In synthesizing the key findings from these analyses, here we provide guidance on best practices for generating and assessing the maturity of hiPSC-CMs with the goal of fostering a transparent discussion toward convergence among the community to progress toward engineering adult-like hiPSC-CMs.

Methodology

Across over 2,000 studies using hiPSC-CMs from 2016 to 2022, there exists high variability in differentiation protocols, maturation strategies and assessment of cell or tissue functionality. To understand the nature of this variability, we systematically analyzed 300 studies using hiPSC-CM models and compiled data on these components. Using a PubMed search for ‘((induced pluripotent stem cells) OR (iPSC)) AND ((cardiomyocyte) OR (cardiomyocytes) OR (iPSC-CM) OR (iPSC-CMs) OR (induced pluripotent stem cell-cardiomyocytes) OR (induced pluripotent stem cell-CMs)) AND ((engineered heart

Table 1 | Adult CM benchmarking parameters and values

Benchmarking parameters and corresponding values of adult CMs/tissues	
Structural organization	<ul style="list-style-type: none"> • Rod shaped with aligned, developed myofibrils • Binucleated¹⁶³ • Sarcomere length: ~2.0–2.2 μm (refs. 164,165) • CM surface area: ~10,000–14,000 μm² (ref. 166) • T-tubules present • Mitochondria localized near sarcomere¹⁶⁷ • Expression of adult ventricular CM-specific structural genes (that is, <i>MYH7</i>, <i>MYL2</i>, <i>TNNI3</i>, and so on)
Mechanical properties	<ul style="list-style-type: none"> • Tissue elastic modulus ~10–50 kPa (ref. 168)
Force	<ul style="list-style-type: none"> • Contractile stress: ~30–60 mN mm⁻² (refs. 169,170) • Positive force–frequency ratio
Electrophysiology	<ul style="list-style-type: none"> • Low-to-zero spontaneous contractions^{24,171} • Characteristic notch at the top of upstroke¹⁶⁶ • RMP: ~–90 mV (ref. 172) • Action potential amplitude: ~100–110 mV (ref. 173) • Action potential duration: ~230–300 ms (ref. 174) • Depolarization velocity: ~250–300 V s⁻¹ (ref. 173) • Conduction velocity: ~30–100 cm s⁻¹ (ref. 25)
Calcium conduction	<ul style="list-style-type: none"> • Cytosolic Ca²⁺ concentration¹⁷⁵ <ul style="list-style-type: none"> • Resting: ~100 nM • Post-sarcoplasmic reticulum calcium release: ~1 μM • Mature sarcoplasmic reticulum function • Increased gene expression of calcium-handling machinery (<i>CACNA1C</i>, <i>SCN5A</i>, <i>KCND3</i>, <i>KCNJ2</i>, <i>SLC8A1</i>, <i>ATP2A2</i>, <i>CASQ2</i>, <i>RYR2</i>, <i>GJA1</i>, <i>PLN</i>) • Robust organization of calcium-handling machinery
Metabolic maturity	<ul style="list-style-type: none"> • Reliant mainly on fatty acid oxidation: >70%^{142,143} • Reduction in glycolysis: <10% of total energy source¹⁴² • Mitochondrial volume: ~30% of cell volume²⁴

tissue) OR (cardiac microtissue) OR (maturation) OR (mature))’; we identified 846 potential publications for analysis. We eliminated publications focusing on atrial differentiation due to relatively limited work in this space and focused our benchmarking on ventricular CMs. We also eliminated publications that were solely focused on disease modeling but included disease-modeling publications in which maturation techniques (the primary focus of our analysis) were used in model development. To capture overall trends in the field, we focused on 300 publications. This included the top 100 cited publications from the 846 potential publications based on citation numbers reported by the Web of Science database as of 2022, 100 randomly selected publications from the potential publications and 100 additional hiPSC-CM publications that were manually selected from references in recent high-impact reviews on cardiac tissue engineering or top search results for ‘iPSC-cardiomyocytes’ on Google Scholar.

After accumulating and analyzing data reported from these publications, we analyzed functional outputs in structural, contractile, calcium-handling, electrophysiology, gene expression and metabolic assessments to identify patterns in the effects of model parameters on cardiac maturation. Graphs depicting functional outputs show mean ± s.e.m. unless otherwise noted. Data were assessed with one-way ANOVA that was corrected for multiple comparisons using a Tukey test with a 95% confidence level. All data used for these analyses can be found in Supplementary Data 1 (ref. 34).

Current approaches to engineer hiPSC-CM in vitro models

hiPSC culture and differentiation

With the widespread adoption of hiPSC-CMs in the field of cardiac tissue engineering, more hiPSC lines are being generated and used in studies to capture global diversity and generate patient-specific models.

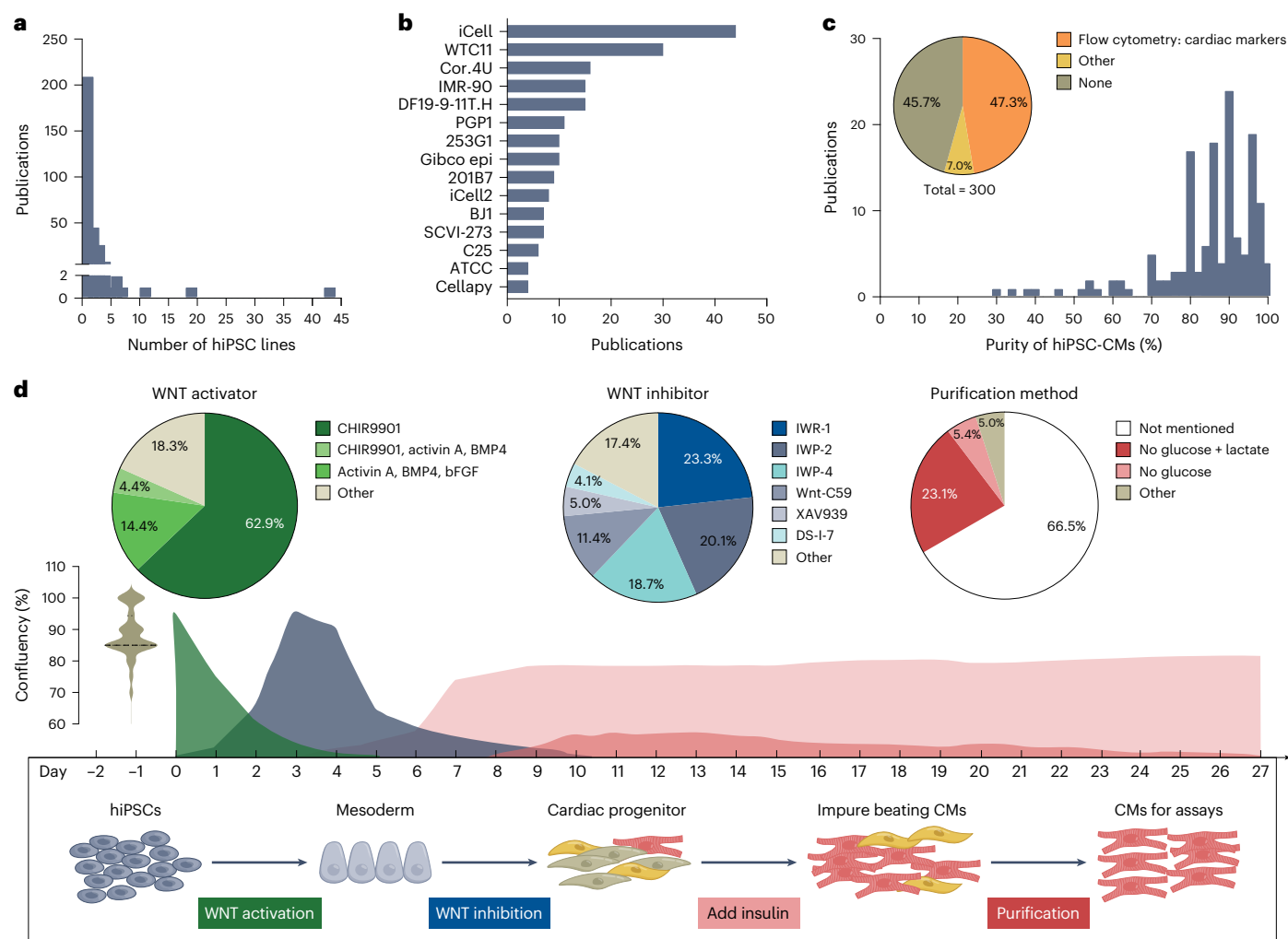


Fig. 1 | hiPSC culture and differentiation. **a**, Histogram of the number of control hiPSC lines that publications reported using for hiPSC-CM differentiation. **b**, Top 15 reported hiPSC lines in the analyzed publications. Gibco epi, Gibco episomal. **c**, Histogram of the reported purity of CMs after hiPSC-CM differentiation. Inset: reported methods of assessing the purity of CMs after hiPSC-CM differentiation. **d**, Schematic of the variability in hiPSC-CM differentiation protocols. Confluency of hiPSCs is typically at ~80–90% at the start of differentiation (day 0) ($n = 108$). There is variability in the time course of WNT pathway activation (green) and

inhibition (blue) in hiPSC-CM differentiation, along with when insulin is added to the medium (pink) and the hiPSC-CM purification method (red). Pie charts represent the top reported WNT pathway activators ($n = 229$), WNT pathway inhibitors ($n = 219$) and purification methods ($n = 300$). n values represent the number of publications that used and reported on each differentiation component. BMP4, bone morphogenetic protein 4; bFGF, basic fibroblast growth factor.

Here, we compiled information on the most commonly used hiPSC lines and hiPSC-CM differentiation protocols within the field.

hiPSC lines. A major source of variability across studies is the choice of hiPSC lines. Over 200 different hiPSC lines were used across the analyzed studies. Over two-thirds of these studies used only one healthy control hiPSC line and thus failed to assess how different hiPSC lines may influence study findings (Fig. 1a). Of the 15 most used hiPSC lines across the papers analyzed (Fig. 1b), two-thirds have a female genetic background and only six have ancestral information available (Supplementary Table 1). Four of these 15 lines are hiPSC lines that are commercially differentiated into CMs (Fig. 1b). Of note, Cor.4U CMs, which were used in 5% of the studies we analyzed, were found to be derived from hESCs, rather than hiPSCs, which are the focus of this Perspective³⁵. The most frequently reported lines that are not commercially differentiated include WTC11, IMR-90, DF19-9-11T.H, PGP1, 253G1, the Gibco episomal line, 201B7, BJ1, SCVI-273, C25 and ATCC (Fig. 1b). It has been shown that the genetic background of hiPSC lines impacts the maintenance of hiPSC pluripotency³⁶ and influences transcriptional

variation³⁷, which could ultimately impact the differentiation and function of derived hiPSC-CMs³⁸, highlighting the importance of including hiPSCs from diverse genetic backgrounds.

hiPSC differentiation into CMs. hiPSC culture medium can also influence the maintenance of hiPSC pluripotency and self-renewal³⁹. Over 55% of publications used one of two commercially available hiPSC culture media as the backbone medium: mTeSR 1 (Stemcell Technologies) or Essential 8 Medium (Gibco) (Supplementary Data 1). During and after differentiation, the backbone culture medium was typically changed to RPMI 1640 (>50%), StemPro-34 (~5%) or those from commercially available kits. Supplements and additives such as B-27 (>50% of publications), L-ascorbic acid, albumin, L-glutamine, HEPES and more were added to some cultures (Supplementary Data 1). Additionally, the matrix (if any) that hiPSCs are seeded on during and after differentiation has been found to impact hiPSC-CM purity and maturation^{40,41}. Matrigel (~30%), gelatin (~20%) and fibronectin (~15%) were the most commonly reported matrices used for hiPSC culture (Supplementary Data 1).

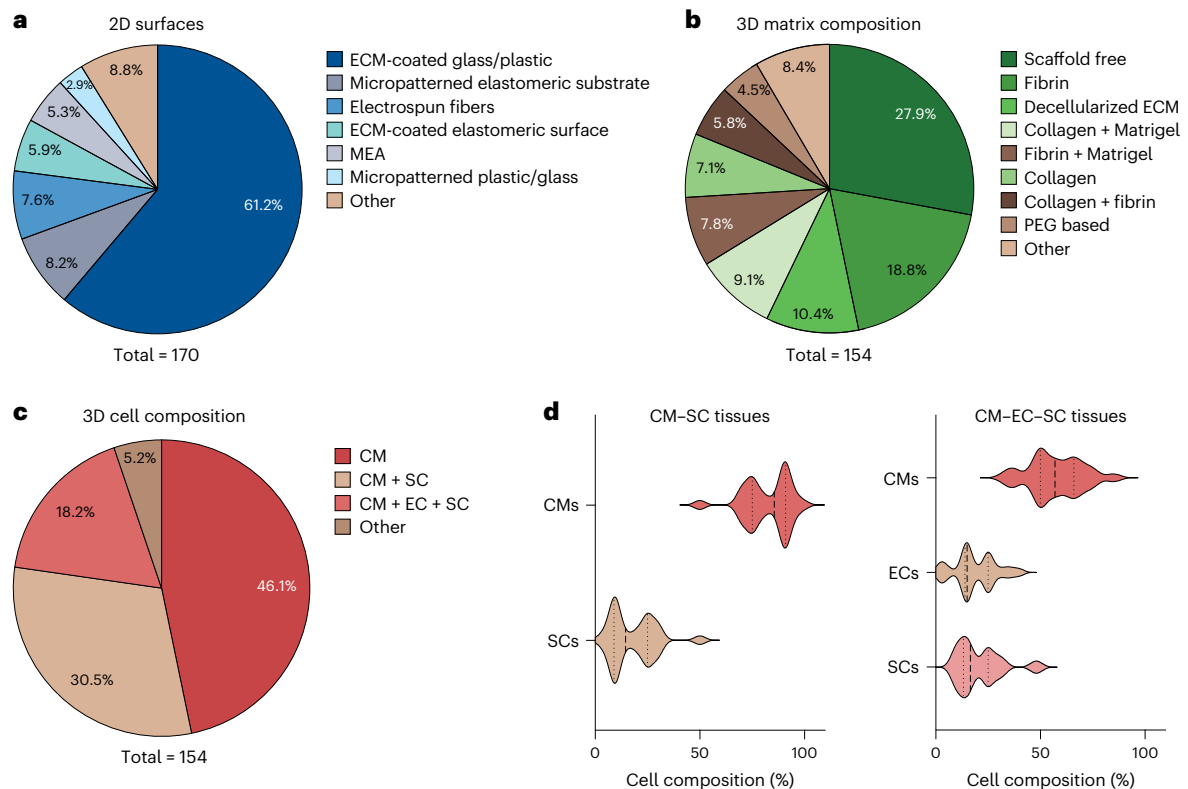


Fig. 2 | Variability in hiPSC-CM platforms. **a**, Top types of substrate platforms that hiPSC-CMs are seeded on in 2D. MEA, multielectrode array. **b**, Top ECM or biomaterial platform used to engineer cardiac microtissues. PEG, polyethylene glycol. **c**, Fraction of cardiac microtissues that are composed of hiPSC-CMs alone (CM), hiPSC-CMs with SCs (CM + SC) or hiPSC-CMs with ECs and SCs (CM + EC + SC). **d**, Left: distribution of CM and SC composition in CM-SC cardiac microtissues ($n = 50$). Right: distribution of CM, EC and SC composition in CM-EC-SC cardiac microtissues ($n = 26$). Dashed and dotted lines represent medians and quartiles, respectively.

While most protocols used to generate CMs are based on temporal modulation of the WNT signaling pathway⁴², adjustments to differentiation parameters are often required for successful CM differentiation across hiPSC lines⁴³ (Fig. 1d). Of the analyzed studies, CHIR9901 was the most commonly employed WNT agonist used to initiate the differentiation process (used in >60% of studies analyzed). CHIR9901 was typically added to hiPSCs at ~80–90% confluency for 24 h from day 0 to about day 1. Subsequent WNT pathway inhibition with IWR-1, IWP-2 or IWP-4 was conducted from approximately day 3 to day 4 of differentiation. Insulin was typically added on day 7 of differentiation. The use of metabolic selection to improve the purity of hiPSC-CMs⁴⁴ was only reported in one-third of the publications. Of these publications, about 70% removed glucose from the medium and supplemented the medium with lactate to starve non-myocytes.

While many studies failed to quantify hiPSC-CM purity after differentiation, over half of the studies reported using either flow cytometry or immunohistochemistry for cardiac-specific markers, such as cardiac troponin T (cTnT) or α -actinin, to quantify the percentage of successfully differentiated hiPSCs (Fig. 1c). The average reported purity of CMs was 84%.

Overall, similar differentiation protocols are used across the field; however, variations in timing and concentration of WNT agonists and antagonists appear to be necessary for successful CM differentiation of different lines⁴³. Additional variability arises from differences in culture techniques across groups. While we acknowledge the challenges associated with controlling for these variables, it would be advantageous for the field to reduce variability in differentiation protocols when possible. As a start, more studies should adopt a common differentiation protocol as a comparator to their group’s traditional protocol and report the purity of their hiPSC-CMs. Purity is important not only

when interpreting studies but also to provide additional assurance that non-CMs are not unknowingly impacting downstream functional outputs. Identifying and reporting the common non-CM cell populations that arise during differentiation could also aid in optimizing differentiation protocols to improve differentiation efficiency.

Platforms used to study hiPSC-CMs

Following the differentiation of hiPSCs into CMs, these cells are typically incorporated into a variety of culture platforms to study their function, ranging from simple, high-throughput platforms to more complex bioreactor-like systems, many of which require engineering expertise and/or the inclusion of additional cell types.

Two-dimensional platforms. A variety of platforms have been used to generate hiPSC-CM models for studying hiPSC-CM maturation, disease progression and drug toxicity. These models can broadly be divided into two-dimensional (2D) versus three-dimensional (3D) tissue platforms. Two-dimensional platforms are more commonly used than 3D tissue platforms due to their accessibility and higher-throughput readouts. Additionally, 2D platforms facilitate the use of imaging and higher-resolution analysis techniques to study CM structure and function. Across both 2D and 3D tissues, the most used culture platform for hiPSC-CMs was extracellular matrix (ECM)-coated glass or plastic substrates (60%) (Fig. 2a). While fibronectin or Matrigel are typically coated onto culture surfaces to facilitate cell adhesion, stromal cell-derived ECM has recently been reported to also improve the maturation of hiPSC-CMs⁴⁰.

Recent improvements to 2D platforms have focused on providing topographical cues to hiPSC-CMs to drive CM alignment, mimicking the organization of the native myocardium. This alignment

has been achieved by culturing CMs on micropatterned rectangles or lines^{21,27,45–55}, electrospun scaffolds composed of aligned polymeric fibers^{56–64}, grooved substrates^{65–70} and 3D-printed anisotropic scaffolds^{71–73}. Additionally, several studies have cultured hiPSC-CMs on elastomeric surfaces that better recapitulate the mechanics of the native myocardium^{74–79}. These substrates are typically made from hydrogels or elastomers, including polyacrylamide^{33–55,80,81} or polydimethylsiloxane (PDMS)^{28,82–84}, respectively. While 2D platforms can provide insights into the effect of specific parameters (that is, substrate stiffness and ligand type and density) on CMs, they are difficult to maintain in long-term culture and do not accurately recapitulate the complex structure and dimensionality of native tissue. Thus, they are limited in their ability to mimic specific aspects of development, physiology and disease.

Three-dimensional platforms. Three-dimensional hiPSC-CM tissues have become more widespread as they more accurately recapitulate the 3D architecture of the cardiac microenvironment in which CMs normally function. The majority of 3D cardiac microtissues studied are considered scaffold free (Fig. 2b). An example of scaffold-free microtissues includes spheroid cultures, which have been used as a high-throughput assay to test the effects of non-CMs on tissue stability and maturation. Other 3D hiPSC-CM tissues require the addition of ECM proteins to facilitate tissue assembly. The most common ECM proteins used include fibrin, collagen, Matrigel or some combination of these materials. Additionally, a handful of groups have explored the use of decellularized ECM^{85–88} and synthetic hydrogels made of materials such as polyethylene glycol^{71,89} to generate cardiac microtissues. Furthermore, the culture medium used to maintain these tissues has a substantial impact on the system, with over 80 combinations of medium components used. More than one-third of the 3D hiPSC-CM models were cultured in medium containing serum, despite its limited translational potential. Three-dimensional hiPSC-CMs are more physiologically relevant overall, but complex fabrication processes and increased sources of variability limit both the accessibility and the throughput of these models.

Another layer of complexity to some 3D cardiac microtissues is the incorporation of supporting cell types. While some 2D hiPSC-CM cultures contained admixed cell types^{90–92}, over 90% of 2D studies used purified hiPSC-CM cultures. By contrast, about half of the 3D hiPSC-CM tissues contained cell types such as mesenchymal stromal cells (SCs) and endothelial cells (ECs) due to either their ability to facilitate tissue compaction or the potential to study the impact of these cell types on cardiac microtissue maturation and function (Fig. 2c). SCs used in these studies include primary cardiac fibroblasts, mesenchymal stem cells, hiPSC-derived cardiac fibroblasts, lung fibroblasts, mural cells, dermal fibroblasts, foreskin fibroblasts, hiPSC-derived stromal cells, hiPSC-derived mural cells, adipose-derived stem cells, pericytes and hiPSC-derived smooth muscle cells. This variability is consequential, as it has been shown that the stromal cell source can impact tissue assembly and functionality⁹³. Additionally, the proportion of stromal cells included, which can impact hiPSC-CM function⁹⁴, varied, but many groups used them in either a 1:9 or 1:3 ratio with hiPSC-CMs (Fig. 2d).

Lastly, many groups have also explored the incorporation of ECs to vascularize and further mature cardiac microtissues (Fig. 2c). Not only does vascularization of cardiac microtissues enable the generation of thicker tissues, but the addition of ECs has also been found to mature CMs via paracrine signaling⁹⁵. Prominent EC sources include hiPSC-derived ECs and primary human umbilical vein ECs. In CM-EC-SC tissues, ECs and SCs were most often included in a 1:1 ratio, with over 50% of the tissue being composed of hiPSC-CMs (Fig. 2d).

Overall, the composition of each platform is influenced by the intended use and resource accessibility. This variability in model design can impact the techniques used to assess resulting tissues and their

maturation. Dissemination of detailed protocols is critical to making complex cardiac microtissue platforms widely accessible, allowing others in the field to apply new techniques to improve the maturation and physiological relevance of their models.

Strategies used to mature hiPSC-CMs

Numerous strategies have been developed to simulate developmental cues found in the native cardiac microenvironment to direct hiPSC-CM maturation toward a more adult-like phenotype (Fig. 3). In this analysis, we grouped these cues into five categories (alignment, mechanical, electrical, co-culture and metabolic maturation techniques) to identify trends in how these techniques are being implemented across the field.

Alignment cues. Given the high degree of alignment of native CMs, alignment cues are common maturation techniques in 2D hiPSC-CM platforms and include micropatterning, aligned electrospun fibrous scaffolds and grooved surfaces at the microscale^{27,53,56,65} and the nanoscale^{58,61,70} (Fig. 3a). Other variables that may contribute to the success of alignment cues in 2D platforms include adhesive ligand and substrate stiffness. Three-dimensional pillar platforms provide alignment via tension, and recent work extended these techniques by bioprinting anisotropic microtissues into larger-scale organized tissue patches⁹⁶.

Mechanical stimulation. Mechanical maturation techniques include the use of passive tension^{96–100}, culturing on hydrogel or elastomeric substrates^{66,101,102}, dynamic mechanical stimulation of tissue^{83,103–107} and the application of shear forces^{108–110} (Fig. 3a). Across all studies analyzed, mechanical cues were the most used maturation technique (Fig. 3b), likely due to the widespread adoption of 2D hydrogel culture platforms as well as 3D engineered heart tissues (EHTs) composed of tissues tethered between two elastomeric pillars (Fig. 2a,b). Elastic hydrogels of physiologically relevant elastic moduli between 3 and 10 kPa have been shown to improve the maturation and function of hiPSC-CMs compared to supraphysiologic, stiff tissue culture plastic or glass^{27,54,102,111}. In EHT platforms, increasing passive tension, or afterload, modulated by pillar stiffness has generally been shown to improve tissue formation, CM alignment and functional maturation^{96,112}. However, too high of an afterload can lead to pathological responses^{113,114}.

Lastly, cyclic mechanical stimulation to mimic the contractile behavior of the heart and pace hiPSC-CMs in 2D or 3D has been achieved using pressure changes^{103,104} and cyclic stretching^{105,106,115}. However, this technique was used sparingly, in less than 7% of the studies we analyzed.

Electrical stimulation. Electrical pacing has shown great improvements in the maturation¹¹⁶ of engineered cardiac microtissue, leading >12% of studies to use this technique (Fig. 3b). Previous work showed that initiating electrical stimulation earlier in hiPSC-CM differentiation and gradually increasing stimulation frequency over time (Fig. 3a) can greatly improve the maturation of EHTs compared to the commonly used constant stimulation of 1 Hz initiated later after EHT assembly¹¹⁶. These electrically paced tissues had adult-like gene expression profiles, increased mitochondrial density, the presence of transverse tubules (t-tubules) and a positive force–frequency relationship.

Co-culture of hiPSC-CMs with other cell types. As heterocellular signaling plays an important role in native tissue development²⁴, there have been notable efforts to characterize the impact of other cell types on hiPSC-CM maturation and overall tissue function. Over 50% of publications incorporated SCs and/or ECs when generating cardiac microtissues (Figs. 2c and 3b), which can improve hiPSC-CM maturation, such as increased formation of t-tubules, contractility and electrophysical

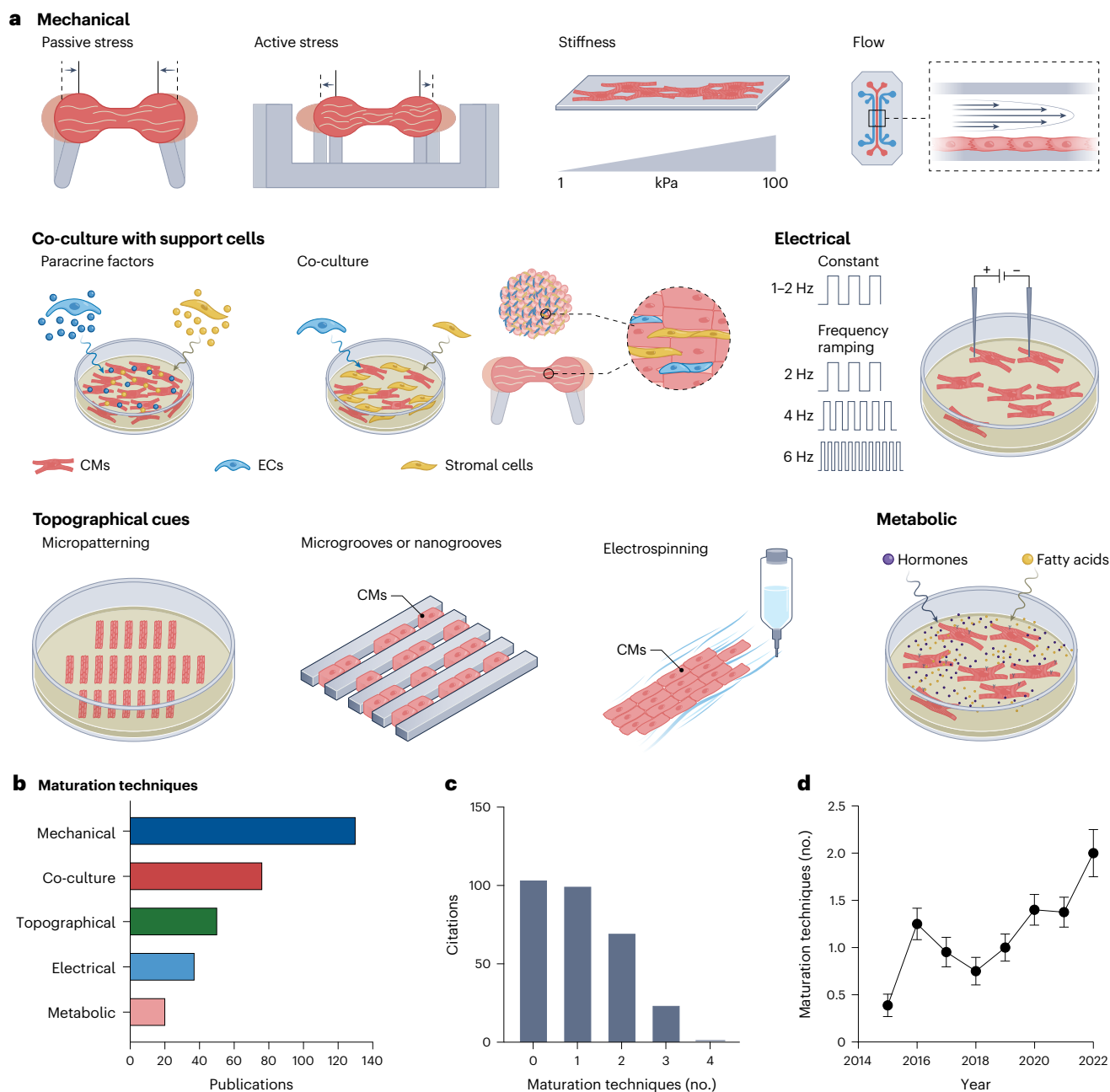


Fig. 3 | Maturation techniques used in hiPSC-CM culture. **a**, Schematic of types of maturation techniques, including mechanical, metabolic, co-culture, electrical stimulation and alignment cues. **b**, Number of publications that reported using the listed maturation techniques. **c**, Histogram of the number of maturation techniques that the analyzed publications reported. **d**, Average number of maturation techniques reported over time ($n = 18-34$). Error bars are s.e.m.

function⁹⁵. Soluble factors from SCs, without physical co-culture, can also improve the maturation of hiPSC-CMs¹¹⁷.

Metabolic maturation. Strategies focusing on metabolic maturation typically employ medium formulations and small molecules that drive a shift from glycolysis to oxidative phosphorylation as the primary source of adenosine triphosphate production in hiPSC-CMs. Studies have shown that the use of triiodothyronine¹¹⁸ and dexamethasone⁷⁸ increases mitochondrial activity and improves contractile performance and calcium handling of hiPSC-CMs. Other studies have shown that the switch from media containing glucose to those containing galactose and fatty acids promotes maturation^{26,119}. Metabolic maturation is a more nascent technique adopted in under 10% of studies; its

ease of implementation makes it likely to be more widely integrated into workflows across laboratories.

Utilization of maturation techniques. Despite maturation techniques generally leading to improvements in the function, robustness and utility of hiPSC-CM models, more than one-third of the studies we analyzed did not use any of these techniques (Fig. 3c). By contrast, many studies combined multiple maturation techniques toward enhancing hiPSC-CM maturation, with about one-third of studies exploring at least two maturation techniques (Fig. 3c). We note a steady increase in the average number of maturation techniques implemented per study from 1.3 in 2016 to 2.0 in 2022 (Fig. 3d). More systematic studies are needed to understand which of these techniques are most successful in driving

specific phenotype changes in hiPSC-CMs and how combinations of techniques may act synergistically to improve maturation.

Metrics to assess hiPSC-CM maturity and function

Identifying techniques that are most effective in driving hiPSC-CM maturation requires robust methods to assess hiPSC-CM function. To quantify which assessment metrics are most commonly used and might best inform overall tissue maturity, we examined commonly reported approaches used to obtain data on the structure and the function of hiPSC-CMs and derivative tissues.

Structural analyses. Over 85% of studies reported data on the morphology and the organization of sarcomeres in hiPSC-CMs or cardiac microtissues, given the critical role of myofibrils in cell contractile function (Fig. 4a). To obtain these metrics, over 60% of studies performed immunostaining, while over 20% of studies used electron microscopy to assess the structure of hiPSC-CMs (Fig. 4b). Proteins that were commonly labeled by immunostaining to visualize hiPSC-CM subcellular structure include cTnT, α -actinin, cardiac troponin I, β -myosin heavy chain and connexin 43. While some studies showed qualitative changes, many used immunostaining of sarcomeric proteins to assess myofibril morphometrics, such as sarcomere length and orientation. There are dozens of published image analysis scripts used to analyze sarcomere alignment with unique approaches in sarcomere segmentation and computing gradients, for example, refs. 120–124. These differing methods lead to many metrics of alignment, including orientation order parameter^{121,122}, dispersion parameter¹²⁴ and the Haralick correlation score¹²³, thereby obfuscating direct comparisons across studies.

Methods of imaging the ultrastructure of hiPSC-CMs mainly focus on identifying key subcellular structural components and their positioning. These features include the relative organization of Z-lines, the I-band, H-zones and M-lines in sarcomeres, the morphology and density of mitochondria and the presence of caveolae. A structural feature that is associated with high levels of maturation of hiPSC-CMs is the presence and orientation of t-tubules, which has been confirmed in numerous recent studies^{31,52,53,78,95,116,125–135}.

Contractility measurements. Contractility measurements were the second most reported metric of analysis, with over half of the studies reporting a contractility measurement (Fig. 4a). In 2D, the most high-throughput and accessible method of obtaining a contractility metric was using video-based analysis to quantify the displacement of hiPSC-CMs during contraction^{27,136}. While this method provides valuable data on contractility kinetics and allows for insight into relative changes in contractility, it does not provide a quantitative value of contractility that can be compared across studies. A more quantitative contractility metric that is used in 2D is sarcomere shortening (the fraction that sarcomeres displace relative to their spacing in a relaxed state)¹²¹. While this quantification method can be more readily compared across studies, it still does not directly quantify the contractile force or stress of the cells and requires live-cell fluorescent labeling of sarcomeres¹³⁷. Traction force microscopy, in which the displacement of fluorescent beads embedded in an elastic hydrogel is tracked over time, can be used to quantify the contractile force and stress of unpatterned or patterned hiPSC-CMs, both at single-cell¹¹¹ and multicellular¹⁶ levels.

Similarly, contractile force and stress of hiPSC-CMs in 3D platforms can be quantified using video motion analysis of the displacement of tissue constraints of known stiffness such as elastomeric pillars¹⁰⁰. Three-dimensional hiPSC-CM tissues also produce enough force to be captured by force transducers. Among the studies we analyzed that reported contraction metrics, over 15% of studies used force transducers (Fig. 4b)^{21,33,135}. To address the variable size of 3D microtissues across and within platforms, contractile stress factoring in tissue geometry should be calculated in addition to force to enable

benchmarking of contractility between various platforms. Additionally, we have noted that, in traditional EHT systems composed of two elastic pillars that both deflect upon tissue contraction, some groups calculate the EHT contractile force by measuring the displacement of one of the pillars, while other groups sum the deflection of the two pillars to obtain a ‘total’ tissue displacement. However, tension within the suspended tissue is applied equally on each post, and thus the tension in the tissue equals the tension applied at one post, not the sum of the tension at both posts. These observations and suggestions highlight the importance of the quantification method in comparing metrics across studies.

Genetic analyses. The next most reported metric was gene expression. Most studies that report gene expression used quantitative polymerase chain reaction with reverse transcription to analyze relative changes in expression of genes predetermined from their study design. A more thorough look at changes in gene expression is now accessible due to many recent innovations in RNA sequencing, in which the average relative changes in expression of all detected genes can be reported, enabling pathway-level analyses to determine changes in cellular signaling underlying CM maturation.

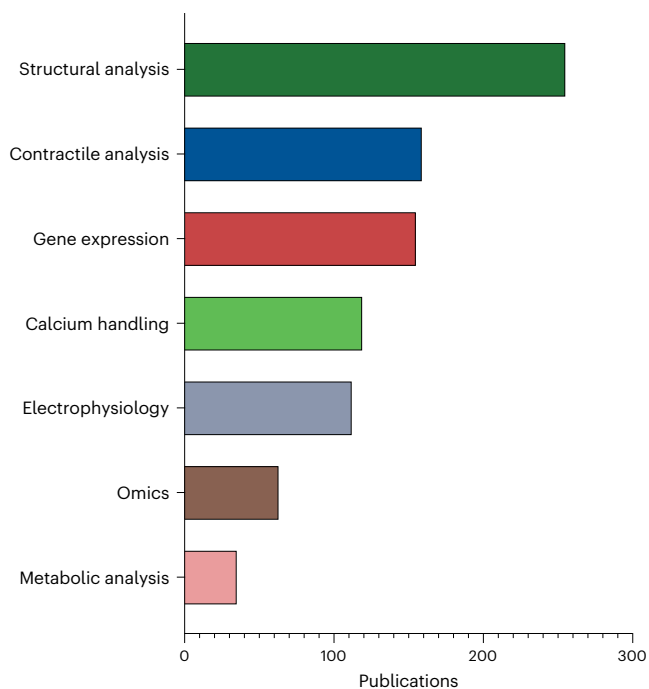
Genes that were most reported include *MYL2*, *MYH7*, *MYH6*, *TNNT2*, *ATP2A2*, *TNNI3*, *RYR2*, *MYL7*, *GJA1*, *NKX2-5*, *PLN*, *CASQ2*, *SCN5A*, *CACNA1C* and *KCNJ2* (Fig. 4c). These genes are associated with pathways and proteins involved in cardiac contraction and electrical conduction. As the composition of CMs evolves during maturation, their expression of different protein isoforms does as well. Oftentimes, the relative expression of genes encoding these isoform transitions is reported to assess improvements in maturation (that is, *MYH7*–*MYH6*, *MYL2*–*MYL7*, *TNNI3*–*TNNI1*).

In addition to gene expression analyses of hiPSC-CM models, over 20% of studies performed other omics analyses. While transcriptomics providing gene expression analyses were the most common, proteomics and metabolomics have also been used recently, often in combination with transcriptomics to better understand transcriptional and translational changes as well as their interrelationship during hiPSC-CM maturation.

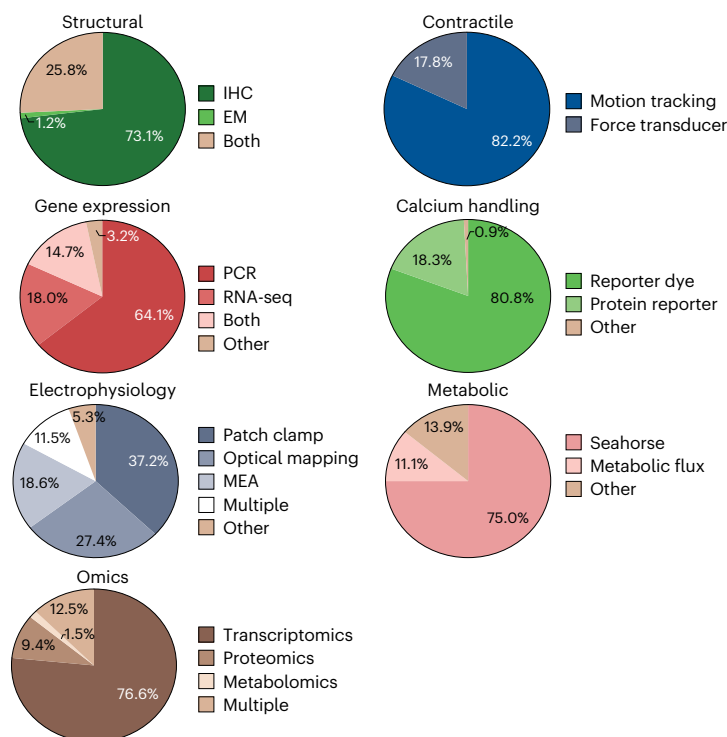
Calcium handling and electrophysiological measurements. Calcium handling and electrophysiological measurements were also common measures of CM function (Fig. 4a), as they are directly related to both the structural and functional maturity of hiPSC-CMs. Calcium handling is most often quantified with calcium-sensitive dyes, such as Rhod-2, Fura-2 AM or Fluo-4 AM, which enable imaging of calcium dynamics via high-speed microscopy (Fig. 4b). Some studies have also implemented genetically encoded calcium indicators, such as GCaMP¹³⁸, to observe calcium transients. Several algorithms have been developed to quantify calcium fluxes^{136,139,140}, and cell-screening systems have implemented software for the high-throughput analysis of calcium handling.

Similarly, electrophysiology can also be quantified by adding voltage-sensitive dyes, such as FluoVolt, di-4-ANEPPS, di-8-ANEPPS or BeRST to CMs, by imaging genetically encoded voltage sensors¹⁴¹ or by directly measuring electrical properties using multielectrode arrays or patch clamping (Fig. 4b). Patch clamping is the gold standard for electrophysical recordings of cells, providing specific electrophysical properties such as RMP that allow for benchmarking of hiPSC-CMs against adult CMs. However, it can be difficult to obtain patch-clamp measurements from 3D cultures, leading many groups to opt for optical mapping via voltage-sensitive dyes to obtain tissue-scale measurements. One of the most reported metrics from both calcium handling and electrophysiological measurements was conduction velocity, which assesses the maturity of the calcium-handling machinery across an entire tissue and the electrical coupling of hiPSC-CMs within the tissue, both of which are critical to the function of myocardial tissue.

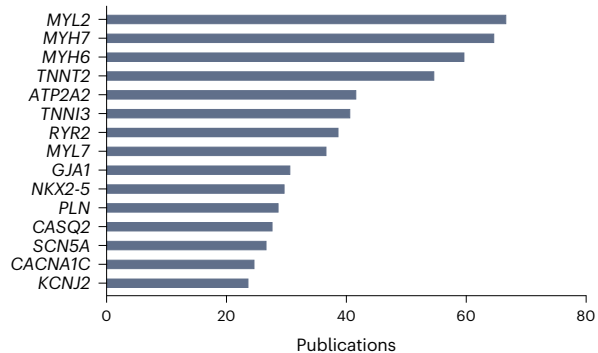
a Reported assessment categories



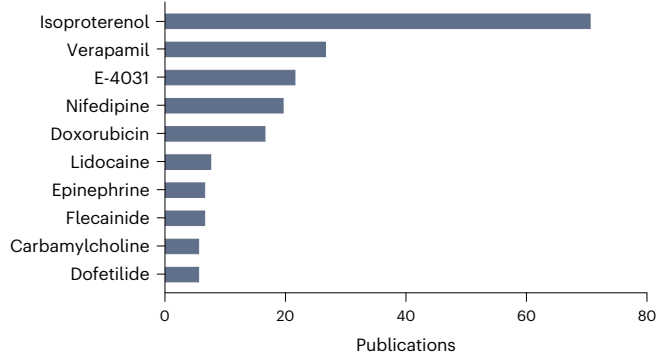
b Assessment methods



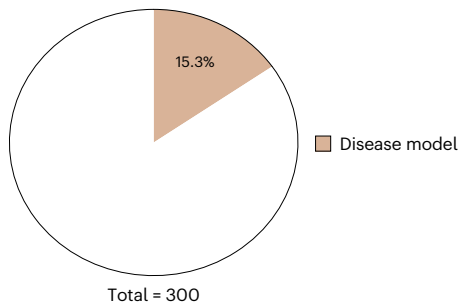
c Top reported genes



d Top reported drugs tested



e



f

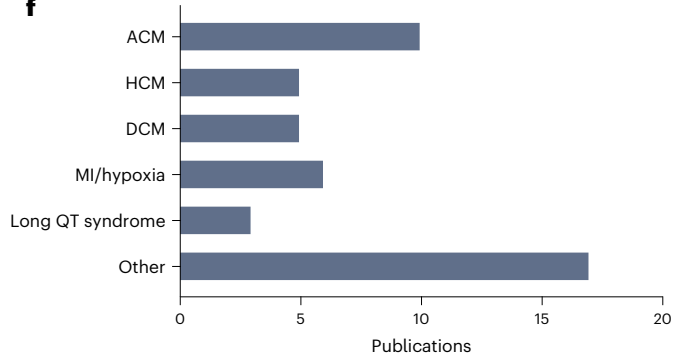


Fig. 4 | Methods of assessing hiPSC-CM functionality and maturation.

a, Number of publications that reported analysis of the structure, contraction, gene expression, calcium handling, electrophysiology and metabolism of hiPSC-CMs. **b**, Top methods of obtaining each of the reported metrics in **a**. EM, electron microscopy; IHC, immunohistochemistry; MEA, microelectrode array; PCR, polymerase chain reaction. **c**, Top genes that were reported in the assessment

of hiPSC-CM maturation. **d**, Top pharmaceutical drugs used to test the ability of hiPSC-CMs to respond as known clinically. **e**, Proportion of publications that used hiPSC-CM platforms to model disease. **f**, Top diseases modeled by hiPSC-CM platforms including ACM, HCM, DCM, myocardial infarction (MI) and long QT syndrome.

Metabolic measurements. A final metric to report on the maturation of hiPSC-CMs is metabolic activity. As metabolic changes in CMs are observed throughout the development of the myocardium, increasing efforts have been made to quantify metabolic activity of hiPSC-CMs to capture the shift from glycolysis to oxidative phosphorylation. Quantifying metabolic activity has become more common in recent years to assess hiPSC-CM maturity, although it was still only used by <15% of studies (Fig. 4a).

The most common assay used to quantify metabolic activity was the Agilent Seahorse assay, which monitors adenosine triphosphate production from glycolytic and oxidative pathways in cultures due to changes in free protons and dissolved oxygen in culture medium (Fig. 4b). Of note, <6% of studies provided a measure reflecting the uptake of fatty acids, the main energy source of mature CMs^{142,143}. Fatty acid uptake was assessed using labeled fatty acids^{26,119} or measuring the oxygen consumption rate with the addition of fatty acids⁷⁰ and/or a fatty acid oxidation inhibitor¹⁴⁴. Many of the publications that assessed metabolism were also focused on developing methods to specifically mature hiPSC-CMs by directly shifting their metabolic activity^{26,119,145,146}, while others used it to assess hiPSC-CM maturation more holistically^{95,116,147}.

Response to cardiac modulatory drugs. A final method for assessing hiPSC-CM maturation was treating cultures with small molecules that are known to impact CM function and quantifying the ability of hiPSC-CMs to respond in a manner reflecting the response of adult CMs (Fig. 4d). Most commonly, the β -adrenergic agonist isoproterenol was added to culture medium to quantify chronotropic and inotropic responses, with a greater contractile force or frequency response indicating increased adrenergic receptors and greater maturity. Other studies used small molecules to determine whether contractility is impaired upon inhibition of specific ion channels found in adult CMs and provide insight into the maturity of the calcium-handling machinery present¹⁴⁸.

Motivation, progress and challenges in hiPSC-CM maturity

Applications of in vitro models requiring improved hiPSC-CM maturity

Drug screening. In addition to using drug challenges to assess the maturity of hiPSC-CM tissues, many models show great potential as mid-to-high-throughput drug-screening platforms. As such, many groups, including regulatory agencies, have begun exploring how patient-specific hiPSC-CM tissues could be used to more accurately identify cardiotoxic effects of therapeutics and ultimately replace expensive and time-consuming in vivo cardiotoxicity assays⁷. However, hiPSC-CMs used for cardiotoxicity testing must be sufficiently mature to ensure that the drug-induced phenotype faithfully represents the cardiac response to the drug in human patients.

For example, verapamil can exhibit false positives in commonly used 2D monolayer toxicity assays, prolonging action potential duration at low doses¹⁴⁹. By treating hiPSC-CMs in 3D culture with maturation medium, these effects were no longer observed at relevant doses, likely due to changes in ion channel expression in more mature tissues. This highlights the necessity to generate mature hiPSC-CMs to accurately assess the potential effectiveness or toxicity of a drug in vitro. However, because many studies did not employ maturation techniques, less mature hiPSC-CMs may be sufficient for testing the efficacy and toxicity of certain drugs, depending on their mechanisms of action (Supplementary Data 1).

Disease modeling. The increased maturation of hiPSC-CM models has also enabled in vitro studies of a multitude of cardiac pathologies. Over 15% of the studies analyzed used hiPSC-CM platforms to model various cardiac pathologies, ACM, HCM, DCM, myocardial infarction and long

QT syndrome (Fig. 4e,f). By using patient-derived or genetically edited hiPSC-CMs or stress-inducing culture conditions, such as hypoxia, studies have been able to model changes in CM structure, contractility and electrophysiology associated with pathology^{16,21,53,114}. Implementing maturation techniques, such as metabolic conditioning, has enabled the recapitulation of key disease phenotypes that were not otherwise prominent in hiPSC-CMs (Fig. 4f)^{21,27,114}. With increasing maturation of hiPSC-CMs, there is growing potential to use these models to shed light on disease mechanisms and potential therapeutic approaches.

Field-level improvements in the maturation of hiPSC-CMs

Despite high variability among maturation techniques and assessment metrics, there were noticeable improvements in frequently assessed metrics (Fig. 5a–d). Sarcomere length, contractile stress and conduction velocity all trended upward over time, suggesting that the field is engineering more mature hiPSC-CMs. Improved measurement tools and techniques could also be contributing to these improvements by enabling more accessible and standardized assessment metrics.

The average reported sarcomere length of hiPSC-CM models increased from $\sim 1.7 \mu\text{m}$ in 2016–2018 to $1.8\text{--}1.9 \mu\text{m}$ in 2020–2021, approaching the sarcomere length of adult CMs, $\sim 2 \mu\text{m}$ (ref. 150) (Fig. 5a). Sarcomere length measurements have been obtained with many different approaches, including the use of different protein markers, imaging techniques and image analyses. Thus, while maturation strategies should lead to improvements in this value, reported values may also be influenced by the employed measurement methods, each of which may have limitations. While some of the highest reported sarcomere lengths are from hiPSC-CM models from studies exploring maturation techniques such as intensity-ramped electrical stimulation¹¹⁶, tricultures¹⁵¹ or patterned elastomeric substrates²⁷, the highest reported average sarcomere length is from a study that did not use any of the maturation techniques assessed here but instead simply cultured hiPSC-CMs for extended periods of time¹²⁹. Extended culture as a technique for hiPSC-CM maturation has also been explored by other groups, but the use of simplistic, 2D culture platforms employed in these studies appears to limit the development of other features of maturation such as t-tubules¹⁵².

Contractile stress, on the other hand, has seen more marked improvements in recent years (Fig. 5b). While the average contractile stress of hiPSC-CM models was 12 mN mm^{-2} (or 12 kPa) in 2021, more recent models have shown contractile stress performance approaching that of adult CMs ($25\text{--}44 \text{ mN mm}^{-2}$ or kPa). These models include a micropillar system with passive tension and co-culture³³ and metabolic maturation on micropatterned substrates²¹. While it appears that the use of maturation techniques is important to the improved contractility of hiPSC-CMs, there was no consensus on best techniques.

Numerous maturation strategies have targeted calcium handling and electrophysiology of hiPSC-CMs. As a result, conduction velocity trended upward in recently published work (Fig. 5c). Multiple models achieved average conduction velocities greater than 30 cm s^{-1} , including models with dynamic mechanical culture²², small molecules targeting signaling pathways³¹, conductive biomaterials⁷⁵, decellularized ECM^{153,154}, human perinatal stem cell-derived ECM⁴⁰, ventricular-specific tissues¹⁵⁵ and 3D-printed tricultures¹⁵⁶.

Despite these improvements, RMP, another common assessment metric, remained stagnant over time at approximately -65 mV with recent decreases toward more adult-like levels (Fig. 5d). This could be, at least in part, because many recent advances have been focused on the development of 3D tissues, in which patch-clamp electrophysiology measurements are difficult to obtain directly. Models that have obtained adult-like RMP, below -80 mV , used dynamical mechanical stretch^{22,114}, ECM-coated elastomeric surfaces^{27,28} and modifications to culture media^{26,30}, all in 2D culture systems. Overall, there is a clear need for improved measurement techniques that accurately assess electrophysiology in 3D tissues.

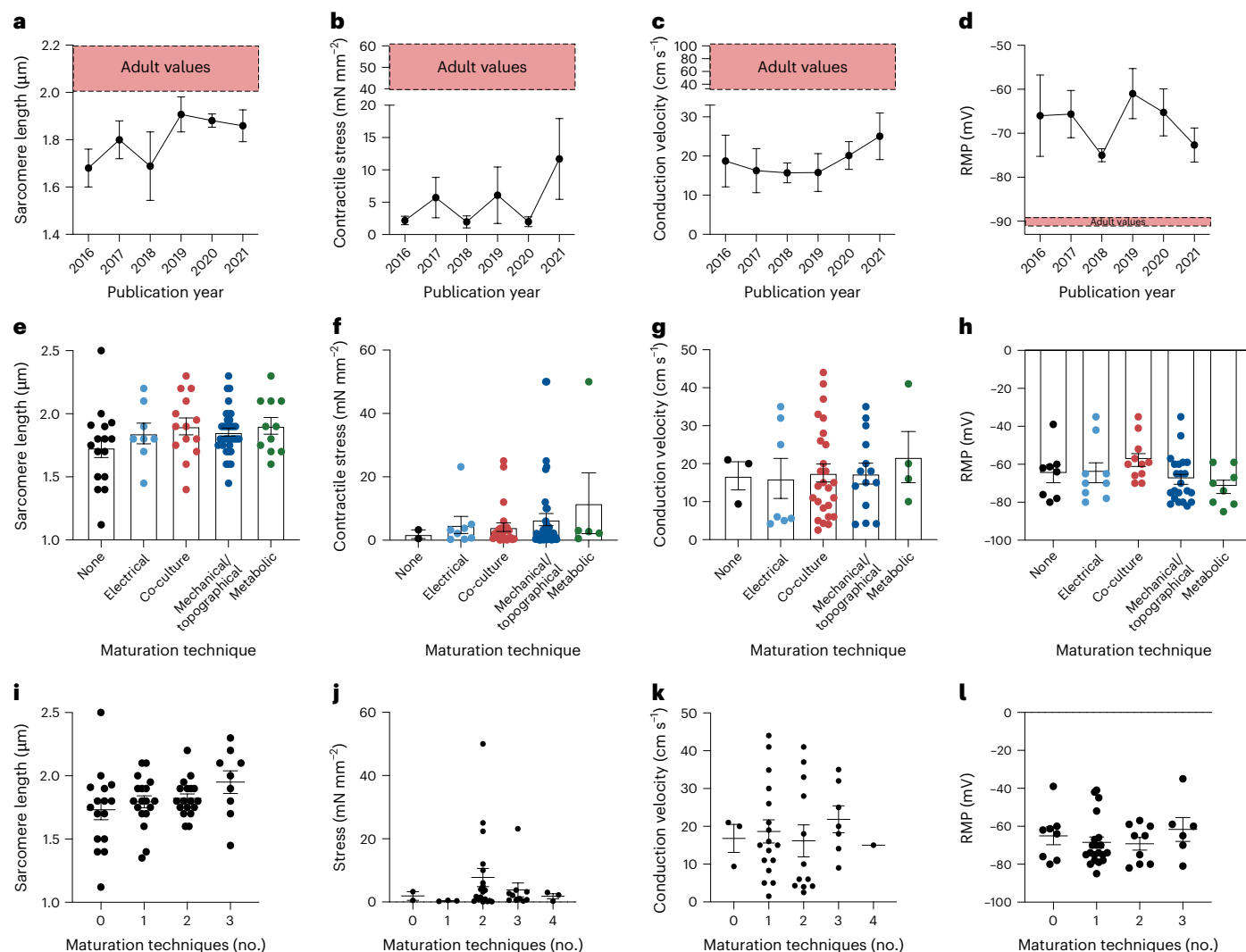


Fig. 5 | Quantification of hiPSC-CM functionality and maturation. **a–d**, Average reported sarcomere length, contractile stress, conduction velocity and RMP in hiPSC-CMs each year from 2016 to 2021 ($n = 4–11$). The years 2015 and 2022 were excluded from these graphs due to limited data availability (analysis was performed mid-2022). Red regions represent values benchmarked

in adult human CMs. **e–h**, Average reported metrics based on types of maturation techniques that were used from all analyzed publications ($n = 2–34$). **i–l**, Average reported metrics based on the number of maturation techniques that were used from all analyzed publications ($n = 2–20$). Maturation techniques were classified as described in Fig. 3. Error bars are s.e.m.

Variability at all levels of hiPSC-CM tissue formation affects maturation outcomes

A major limitation in the field is difficulty in parsing the individual impacts of each maturation technique due to confounding variables present at all levels of engineering hiPSC-CM tissues. Overall, we found no statistically significant differences in sarcomere length, contractile stress, conduction velocity and RMP due to the type of maturation technique (Fig. 5f–h). Additionally, using a greater number of maturation techniques did not improve hiPSC-CM performance (Fig. 5i–l). For this analysis, maturation techniques were grouped as described in Fig. 3. For instance, tissues formed between elastomeric pillars with stromal cells to aid in compaction would be considered to have used two maturation techniques. Thus, while individual studies have shown improvements in hiPSC-CM maturation compared to internal study controls, field-level findings do not reflect this.

Surprisingly, hiPSC-CMs matured with electrical stimulation did not perform as well as hiPSC-CMs matured with other approaches. There are many variables that contribute to differences in electrical stimulation protocols across studies, including the time between differentiation initiation and the beginning of stimulation, stimulation

duration and electrical pulse voltage, width and frequency. For example, one study showed that constant high-frequency stimulation at 3 Hz leads to mitochondrial dysfunction and increased apoptosis in hiPSC-CMs, while low-frequency stimulation at 1 Hz did not¹⁵⁷. Another study showed that intensity-ramped frequencies improved the maturation of hiPSC-CMs, likely due to beneficial effects of mimicking the changes in electromechanical loading that occur during the fetal–postnatal transition of CMs¹¹⁶.

While it is clear from study-specific experimental controls that maturation techniques exert a positive effect, it is also difficult to parse the individual impacts of each maturation technique because of the numerous variables involved. However, variables at multiple levels prevent comparisons of outcomes across studies and therefore also limit convergence on the most promising maturation strategies.

Collective outlook for improved hiPSC-CM maturation

To begin to rigorously assess progress as a field, we have created an accessible database with the protocol parameters and the functional outputs of the 300 studies reported here. These data will allow

researchers to determine current trends more easily within the field, directly compare studies and extract the information needed to replicate a study³⁴. We urge researchers to continue to incorporate data from additional publications so that it can stay current and provide a forum for coordinating progress.

The knowledge gained from compiling this database should subsequently be used to design comprehensive studies that directly compare current maturation techniques to improve the function and the reproducibility of hiPSC-CM models. One way to bypass the influence of protocol variability in determining which maturation techniques are most effective is through a series of studies directly comparing maturation techniques using the same few hiPSC lines within the same platform, culture conditions, measurement techniques and assessment metrics. This would allow the field to gain a better understanding of which components of the CM are most responsive to a given stimulation and how changes impact different aspects of cell or cardiac tissue function. Furthermore, measuring the same metrics with the same techniques and software at the same time point is necessary for direct comparisons of hiPSC-CM functionality.

In addition, there are many other parameters that have been understudied as potentially important factors to systematically investigate. For example, there are many different ECM and ECM-like components used in hiPSC-CM models¹⁵⁸, but there are very few studies investigating the effects of this variable on hiPSC-CM functionality^{159,160}. Many protocols across the field are used by only one or a handful of groups and are not systematically compared to other existing protocols. As such, we do not have sufficient data to identify which variables presented yield the best results, which in turn hampers the field from progressing.

To benchmark new approaches against prior literature and future studies, researchers should use the same control to report on a predetermined set of metrics. One study directly compared hiPSC-CMs derived from ten different lines and showed wide variability in functional outputs within the same EHT platform³⁸. To address this variability, each new study could compare functional properties of hiPSC-CM models to those of the same cell line, perhaps commercially available hiPSC-CMs that come as predifferentiated CMs, minimizing variability that arises from different differentiation protocols. Experimental techniques, such as maturation medium or electrical stimulation, should be tested on hiPSC-CMs in a dish as well as in the engineered platform to separate the effects of experimental techniques from that of the platform on hiPSC-CM maturation. In addition to a shared control line, studies focused on improving hiPSC-CM maturity should use at least five hiPSC-CM lines to test the consistency of their protocols. Far more lines should be included when reporting pharmaceutical and therapeutic effects, including a representative number of lines from different sexes and ancestral backgrounds to account for the potential variability in hiPSC-CM responses. There are increasing efforts to establish and share hiPSC lines from different sexes and ancestral backgrounds¹⁶¹ that should be further utilized.

While we have highlighted the abundance of metrics used to assess hiPSC-CM structure and function, we propose converging on a few essential metrics that are widely accessible using the same methodology to enable direct comparisons across studies and laboratories. Some of the most reported metrics that provide important insight into hiPSC-CM maturation include sarcomere and myofibril morphometrics, contractile stress, conduction velocity and gene expression. Some metrics are highly sensitive to the specific image analysis pipeline used. Thus, it would be critical to develop and jointly adopt open-source analysis pipelines that robustly handle data generated from a range of different platforms to enable direct comparison of data across experiments and laboratories. Furthermore, we encourage the use of voltage-sensitive dyes, such as FluoVolt or di-4-ANEPPS, or calcium-sensitive dyes, such as Fluo-4 AM, to report conduction velocity¹⁶². Additionally, hiPSC-CMs should be electrically paced during calcium-handling analysis to reduce variability in

calcium-handling metrics resulting from inconsistent spontaneous contractions of immature hiPSC-CMs. Lastly, gene expression ratios of key maturation-related genes, such as *MYH7:MYH6*, *MYL2:MYL7* and *TNNI3:TNNI1*, should be reported.

Implementing common analysis software and experimental controls in future experiments and subsequently updating our database with these new results will facilitate the growth of a resource that can be mined using machine learning and high-dimensional data analysis techniques. Analyzing a more comprehensive dataset using such techniques could glean valuable insights into the effects of specific maturation techniques or combinations thereof on maturation outcomes. While the current dataset presented here is currently the most comprehensive analysis in this space, the lack of consistency among studies and the limited number of comparable data points make such analyses quite challenging. As such, once a more comprehensive dataset can be compiled, these techniques and others could be leveraged to extract information that can guide continued progress of the field toward generating mature hiPSC-CMs and derivative cardiac tissue.

While we focus on *in vitro* hiPSC-CM models, much of the insights from this analysis can be used to inform *in vivo* implantation of hiPSC-CM-based tissue patches or cardiac regeneration studies using animal models^{22–24}. Delivery and implantation of hiPSC-CMs *in vivo* has made great progress, showing improved function in the injured heart^{22,23}; however, this introduces additional variables and complex outputs to assess, such as host integration and system-wide functional changes. Similar comprehensive benchmarking of the potential variables inherent to these complex experiments, like the analysis conducted on *in vitro* hiPSC-CM systems presented here, is necessary and would greatly move the field forward. Additionally, while *in vitro* tissue platforms have great potential to model disease and expedite the drug discovery process, synergizing findings from these platforms with animal models or patient samples is critical toward gaining a comprehensive understanding of cardiac pathophysiology. More specifically, it may be necessary to verify findings from reductionist *in vitro* models in more complex *in vivo* settings before moving forward with specific disease-modeling studies, for example. Additionally, due to their increased complexity, various animal models can provide unique insights into specific processes important in cardiac development, regeneration and disease progression and thus should be used to inform the design of novel *in vitro* models.

The multidisciplinary nature of the cardiac tissue-engineering field brings together clinicians, biologists and engineers. Providing researchers from diverse perspectives with a standardized venue to report their findings will allow them to learn from each other and move forward more efficiently. These types of analyses will allow the field to streamline advances in developing models for drug discovery and therapies for cardiac pathologies.

Conclusion

In recent years, there has been substantial progress in the field of cardiac tissue engineering toward generating mature tissues composed of hiPSC-CMs for use as disease models and drug-screening platforms. However, quantitatively benchmarking progress across the field has proved challenging due to variability in many aspects of tissue formation, culture and subsequent assessment, including the choice of hiPSC lines, differentiation protocols for generating CMs, platforms for forming tissues, maturation techniques and various measurements used to assess cell or tissue function. Given the many sources of variability at multiple levels, it is difficult to ascertain which techniques are most effective in improving the maturation of hiPSC-CMs or derivative tissues formed from these cells. Here, we highlight the need for convergence on controls and quantitative analysis methods that will enable more efficient progress toward generating hiPSC-CM tissues that recapitulate adult cardiac physiology with utility for numerous applications. Furthermore, we have made all data used in this analysis

freely accessible and encourage others in the field to contribute to and use this database to better inform their ongoing research and support the collective advancement of the field as a whole³⁴.

Data availability

The data supporting the findings of this field-wide analysis are available within the paper and its Supplementary Information. Additionally, the dataset has been deposited at Dryad and will continue to be updated as new manuscripts are published in this area of research (<https://doi.org/10.5061/dryad.ksn02v7bh>)³⁴.

References

- Wouters, O. J., McKee, M. & Luyten, J. Estimated research and development investment needed to bring a new medicine to market, 2009–2018. *JAMA* **323**, 844–853 (2020).
- Varga, Z. V., Ferdinandy, P., Liaudet, L. & Pacher, P. Drug-induced mitochondrial dysfunction and cardiotoxicity. *Am. J. Physiol. Heart Circ. Physiol.* **309**, H1453–H1467 (2015).
- Bird, S. D. et al. The human adult cardiomyocyte phenotype. *Cardiovasc. Res.* **58**, 423–434 (2003).
- Milani-Nejad, N. & Janssen, P. M. L. Small and large animal models in cardiac contraction research: advantages and disadvantages. *Pharmacol. Ther.* **14**, 235–249 (2014).
- Maltsev, V. A., Rohwedel, J., Hescheler, J. & Wobus, A. M. Embryonic stem cells differentiate in vitro into cardiomyocytes representing sinusnodal, atrial and ventricular cell types. *Mech. Dev.* **44**, 41–50 (1993).
- Takahashi, K. et al. Induction of pluripotent stem cells from adult human fibroblasts by defined factors. *Cell* **131**, 861–872 (2007).
- Colatsky, T. et al. The Comprehensive in Vitro Proarrhythmia Assay (CiPA) initiative — update on progress. *J. Pharmacol. Toxicol. Methods* **81**, 15–20 (2016).
- McKenna, W. J. & Judge, D. P. Epidemiology of the inherited cardiomyopathies. *Nat. Rev. Cardiol.* **18**, 22–36 (2021).
- Ho, C. Y. et al. Genotype and lifetime burden of disease in hypertrophic cardiomyopathy: insights from the Sarcomeric Human Cardiomyopathy Registry (SHaRe). *Circulation* **138**, 1387–1398 (2018).
- Lippi, M. et al. Spectrum of rare and common genetic variants in arrhythmogenic cardiomyopathy patients. *Biomolecules* **12**, 1043 (2022).
- Haas, J. et al. Atlas of the clinical genetics of human dilated cardiomyopathy. *Eur. Heart J.* **36**, 1123–1135 (2015).
- Bhagwan, J. R. et al. Isogenic models of hypertrophic cardiomyopathy unveil differential phenotypes and mechanism-driven therapeutics. *J. Mol. Cell. Cardiol.* **145**, 43–53 (2020).
- Mosqueira, D. et al. CRISPR/Cas9 editing in human pluripotent stem cell-cardiomyocytes highlights arrhythmias, hypocontractility, and energy depletion as potential therapeutic targets for hypertrophic cardiomyopathy. *Eur. Heart J.* **39**, 3879–3892 (2018).
- Loiben, A. M. et al. Cardiomyocyte apoptosis is associated with contractile dysfunction in stem cell model of MYH7 E848G hypertrophic cardiomyopathy. *Int. J. Mol. Sci.* **24**, 4909 (2023).
- Prondzynski, M. et al. Disease modeling of a mutation in α -actinin 2 guides clinical therapy in hypertrophic cardiomyopathy. *EMBO Mol. Med.* **11**, e11115 (2019).
- Zhang, K. et al. Plakophilin-2 truncating variants impair cardiac contractility by disrupting sarcomere stability and organization. *Sci. Adv.* **7**, eabh3995 (2021).
- Cohn, R. et al. A contraction stress model of hypertrophic cardiomyopathy due to sarcomere mutations. *Stem Cell Reports* **12**, 71–83 (2019).
- Hinson, J. T. et al. Titin mutations in iPSC cells define sarcomere insufficiency as a cause of dilated cardiomyopathy. *Science* **349**, 982–986 (2015).
- Toepfer, C. N. et al. Myosin sequestration regulates sarcomere function, cardiomyocyte energetics, and metabolism, informing the pathogenesis of hypertrophic cardiomyopathy. *Circulation* **141**, 828–842 (2020).
- Briganti, F. et al. iPSC modeling of RBM20-deficient DCM identifies upregulation of RBM20 as a therapeutic strategy. *Cell Rep.* **32**, 108117 (2020).
- Knight, W. E. et al. Maturation of pluripotent stem cell-derived cardiomyocytes enables modeling of human hypertrophic cardiomyopathy. *Stem Cell Reports* **16**, 519–533 (2021).
- An informative study using a combination of metabolic maturation and micropatterned surfaces to improve the maturation of hiPSC-CMs, increasing sensitivity to pathological stimuli.**
- Querdel, E. et al. Human engineered heart tissue patches remuscularize the injured heart in a dose-dependent manner. *Circulation* **143**, 1991–2006 (2021).
- An informative study using dynamic mechanical stimulation of EHT patches to obtain improved maturation of hiPSC-CMs. Transplantation of the patches resulted in partial remuscularization of the injured heart in a guinea pig injury model.**
- Liu, Y. W. et al. Human embryonic stem cell-derived cardiomyocytes restore function in infarcted hearts of non-human primates. *Nat. Biotechnol.* **36**, 597–605 (2018).
- Karbassi, E. et al. Cardiomyocyte maturation: advances in knowledge and implications for regenerative medicine. *Nat. Rev. Cardiol.* **17**, 341–359 (2020).
- A comprehensive review on the structural and functional characteristics of mature CMs.**
- Yang, X., Pabon, L. & Murry, C. E. Engineering adolescence: maturation of human pluripotent stem cell-derived cardiomyocytes. *Circ. Res.* **114**, 511–523 (2014).
- Feyen, D. A. M. et al. Metabolic maturation media improve physiological function of human iPSC-derived cardiomyocytes. *Cell Rep.* **32**, 107925 (2020).
- An informative study using metabolic maturation techniques in 2D and 3D, obtaining improved functional maturation of hiPSC-CMs.**
- Tsan, Y. C. et al. Physiologic biomechanics enhance reproducible contractile development in a stem cell derived cardiac muscle platform. *Nat. Commun.* **12**, 6167 (2021).
- An informative study using micropatterning on elastomer substrates to define tissue biomechanics and improve the maturation of hiPSC-CMs.**
- Herron, T. J. et al. Extracellular matrix-mediated maturation of human pluripotent stem cell-derived cardiac monolayer structure and electrophysiological function. *Circ. Arrhythm. Electrophysiol.* **9**, e003638 (2016).
- Martella, D. et al. Liquid crystalline networks toward regenerative medicine and tissue repair. *Small* **13**, 1702677 (2017).
- Lin, B. et al. Culture in glucose-depleted medium supplemented with fatty acid and 3,3',5-triiodo-L-thyronine facilitates purification and maturation of human pluripotent stem cell-derived cardiomyocytes. *Front. Endocrinol.* **8**, 253 (2017).
- Miki, K. et al. ERR γ enhances cardiac maturation with t-tubule formation in human iPSC-derived cardiomyocytes. *Nat. Commun.* **12**, 3596 (2021).
- Mulieri, L. A., Hasenfuss, G., Leavitt, B., Allen, P. D. & Alpert, N. R. Altered myocardial force–frequency relation in human heart failure. *Circulation* **85**, 1743–1750 (1992).
- Melby, J. A. et al. Functionally integrated top–down proteomics for standardized assessment of human induced pluripotent stem cell-derived engineered cardiac tissues. *J. Proteome Res.* **20**, 1424–1433 (2021).

- An informative study establishing a method allowing for the sequential assessment of functional properties and top-down proteomics for hiPSC-engineered cardiac tissue.**
34. Ewoldt, J. K. and DePalma, S.J. et al. Induced pluripotent stem cell-derived cardiomyocyte in vitro models: tissue fabrication protocols, assessment methods, and quantitative maturation metrics for benchmarking progress. *Dryad* <https://doi.org/10.5061/dryad.ksn02v7bh> (2024).
35. Lapp, H. et al. Author Correction: Frequency-dependent drug screening using optogenetic stimulation of human iPSC-derived cardiomyocytes. *Sci. Rep.* **11**, 1643 (2021).
36. Schnabel, L. V., Abratte, C. M., Schimenti, J. C., Southard, T. L. & Fortier, L. A. Genetic background affects induced pluripotent stem cell generation. *Stem Cell Res. Ther.* **3**, 30 (2012).
37. Rouhani, F. et al. Genetic background drives transcriptional variation in human induced pluripotent stem cells. *PLoS Genet.* **10**, e1004432 (2014).
38. Mannhardt, I. et al. Comparison of 10 control hPSC lines for drug screening in an engineered heart tissue format. *Stem Cell Reports* **15**, 983–998 (2020).
- An informative study comparing ten different control hiPSC-CM lines in EHT to demonstrate large baseline cell line-dependent differences in tissue function.**
39. Marinho, P. A., Chailangkarn, T. & Muotri, A. R. Systematic optimization of human pluripotent stem cells media using design of experiments. *Sci. Rep.* **5**, 9834 (2015).
40. Block, T. et al. Human perinatal stem cell derived extracellular matrix enables rapid maturation of hiPSC-CM structural and functional phenotypes. *Sci. Rep.* **10**, 19071 (2020).
41. Zhang, J. et al. Cardiac differentiation of human pluripotent stem cells using defined extracellular matrix proteins reveals essential role of fibronectin. *eLife* **11**, e69028 (2022).
42. Lian, X. et al. Robust cardiomyocyte differentiation from human pluripotent stem cells via temporal modulation of canonical Wnt signaling. *Proc. Natl Acad. Sci. USA* **109**, E1848–E1857 (2012).
43. Mummery, C. L. et al. Differentiation of human embryonic stem cells and induced pluripotent stem cells to cardiomyocytes: a methods overview. *Circ. Res.* **111**, 344–358 (2012).
44. Tohyama, S. et al. Distinct metabolic flow enables large-scale purification of mouse and human pluripotent stem cell-derived cardiomyocytes. *Cell Stem Cell* **12**, 127–137 (2013).
45. Xu, C. et al. Bioinspired onion epithelium-like structure promotes the maturation of cardiomyocytes derived from human pluripotent stem cells. *Biomater. Sci.* **5**, 1810–1819 (2017).
46. Ma, Z. et al. Self-organizing human cardiac microchambers mediated by geometric confinement. *Nat. Commun.* **6**, 7413 (2015).
47. Schulz, A. et al. Tyramine-conjugated alginate hydrogels as a platform for bioactive scaffolds. *J. Biomed. Mater. Res. A* **107**, 114–121 (2019).
48. Hart, C. et al. Rapid nanofabrication of nanostructured interdigitated electrodes (NIDES) for long-term in vitro analysis of human induced pluripotent stem cell differentiated cardiomyocytes. *Biosensors* **8**, 88 (2018).
49. Sun, S. et al. Progressive myofibril reorganization of human cardiomyocytes on a dynamic nanotopographic substrate. *ACS Appl. Mater. Interfaces* **12**, 21450–21462 (2020).
50. Martewicz, S. et al. Transcriptomic characterization of a human in vitro model of arrhythmogenic cardiomyopathy under topological and mechanical stimuli. *Ann. Biomed. Eng.* **47**, 852–865 (2019).
51. Kujala, V. J., Pasqualini, F. S., Goss, J. A., Nawroth, J. C. & Parker, K. K. Laminar ventricular myocardium on a microelectrode array-based chip. *J. Mater. Chem. B* **4**, 3534–3543 (2016).
52. Pioner, J. M. et al. Isolation and mechanical measurements of myofibrils from human induced pluripotent stem cell-derived cardiomyocytes. *Stem Cell Reports* **6**, 885–896 (2016).
53. Strimaityte, D. et al. Contractility and calcium transient maturation in the human iPSC-derived cardiac microfibers. *ACS Appl. Mater. Interfaces* **14**, 35376–35388 (2022).
54. Wheelwright, M. et al. Investigation of human iPSC-derived cardiac myocyte functional maturation by single cell traction force microscopy. *PLoS ONE* **13**, e0194909 (2018).
55. Kit-Anan, W. et al. Multiplexing physical stimulation on single human induced pluripotent stem cell-derived cardiomyocytes for phenotype modulation. *Biofabrication* **13**, 025004 (2021).
56. Wanjare, M. et al. Anisotropic microfibrillar scaffolds enhance the organization and function of cardiomyocytes derived from induced pluripotent stem cells. *Biomater. Sci.* **5**, 1567–1578 (2017).
57. Kumar, N. et al. Scalable biomimetic coaxial aligned nanofiber cardiac patch: a potential model for ‘clinical trials in a dish’. *Front. Bioeng. Biotechnol.* **8**, 567842 (2020).
58. Depalma, S. J., Davidson, C. D., Stis, A. E., Helms, A. S. & Baker, B. M. Microenvironmental determinants of organized iPSC-cardiomyocyte tissues on synthetic fibrous matrices. *Biomater. Sci.* **9**, 93–107 (2021).
59. Li, J. et al. Extracellular recordings of patterned human pluripotent stem cell-derived cardiomyocytes on aligned fibers. *Stem Cells Int.* **2016**, 2634013 (2016).
60. Chun, Y. W. et al. Combinatorial polymer matrices enhance in vitro maturation of human induced pluripotent stem cell-derived cardiomyocytes. *Biomaterials* **67**, 52–64 (2015).
61. Khan, M. et al. Evaluation of changes in morphology and function of human induced pluripotent stem cell derived cardiomyocytes (hiPSC-CMs) cultured on an aligned-nanofiber cardiac patch. *PLoS ONE* **10**, e0126338 (2015).
62. Pushp, P. et al. Functional comparison of beating cardiomyocytes differentiated from umbilical cord-derived mesenchymal/stromal stem cells and human foreskin-derived induced pluripotent stem cells. *J. Biomed. Mater. Res. A* **108**, 496–514 (2020).
63. Chen, Y., Chan, J. P. Y., Wu, J., Li, R. K. & Santerre, J. P. Compatibility and function of human induced pluripotent stem cell derived cardiomyocytes on an electrospun nanofibrillar scaffold, generated from an ionomeric polyurethane composite. *J. Biomed. Mater. Res. A* **110**, 1932–1943 (2022).
64. Tang, Y. et al. Induction and differentiation of human induced pluripotent stem cells into functional cardiomyocytes on a compartmented monolayer of gelatin nanofibers. *Nanoscale* **8**, 14530–14540 (2016).
65. Takada, T. et al. Aligned human induced pluripotent stem cell-derived cardiac tissue improves contractile properties through promoting unidirectional and synchronous cardiomyocyte contraction. *Biomaterials* **281**, 121351 (2022).
66. Pioner, J. M. et al. Optical investigation of action potential and calcium handling maturation of hiPSC-cardiomyocytes on biomimetic substrates. *Int. J. Mol. Sci.* **20**, 3799 (2019).
67. Huethorst, E. et al. Customizable, engineered substrates for rapid screening of cellular cues. *Biofabrication* **12**, 025009 (2020).
68. Carson, D. et al. Nanotopography-induced structural anisotropy and sarcomere development in human cardiomyocytes derived from induced pluripotent stem cells. *ACS Appl. Mater. Interfaces* **8**, 21923–21932 (2016).
69. Smith, A. S. T. et al. NanoMEA: a tool for high-throughput, electrophysiological phenotyping of patterned excitable cells. *Nano Lett.* **20**, 1561–1570 (2020).
70. Afzal, J. et al. Cardiac ultrastructure inspired matrix induces advanced metabolic and functional maturation of differentiated human cardiomyocytes. *Cell Rep.* **40**, 111146 (2022).

71. Cui, H. et al. 4D physiologically adaptable cardiac patch: a 4-month in vivo study for the treatment of myocardial infarction. *Sci. Adv.* **6**, eabb5067 (2020).
72. Zhang, Y. S. et al. Bioprinting 3D microfibrillar scaffolds for engineering endothelialized myocardium and heart-on-a-chip. *Biomaterials* **110**, 45–59 (2016).
73. Gao, L. et al. Myocardial tissue engineering with cells derived from human-induced pluripotent stem cells and a native-like, high-resolution, 3-dimensionally printed scaffold. *Circ. Res.* **120**, 1318–1325 (2017).
74. Feaster, T. K., Casciola, M., Narkar, A. & Blinova, K. Acute effects of cardiac contractility modulation on human induced pluripotent stem cell-derived cardiomyocytes. *Physiol. Rep.* **9**, e15085 (2021).
75. Lind, J. U. et al. Instrumented cardiac microphysiological devices via multimaterial three-dimensional printing. *Nat. Mater.* **16**, 303–308 (2017).
76. Jia, J. et al. Development of peptide-functionalized synthetic hydrogel microarrays for stem cell and tissue engineering applications. *Acta Biomater.* **45**, 110–120 (2016).
77. Park, S. J. et al. Insights into the pathogenesis of catecholaminergic polymorphic ventricular tachycardia from engineered human heart tissue. *Circulation* **140**, 390–404 (2019).
78. Parikh, S. S. et al. Thyroid and glucocorticoid hormones promote functional t-tubule development in human-induced pluripotent stem cell-derived cardiomyocytes. *Circ. Res.* **121**, 1323–1330 (2017).
79. Garbern, J. C. et al. Inhibition of mTOR signaling enhances maturation of cardiomyocytes derived from human-induced pluripotent stem cells via p53-induced quiescence. *Circulation* **141**, 285–300 (2020).
80. Pasqualini, F. S., Sheehy, S. P., Agarwal, A., Aratyn-Schaus, Y. & Parker, K. K. Structural phenotyping of stem cell-derived cardiomyocytes. *Stem Cell Reports* **4**, 340–347 (2015).
81. Buikema, J. W. et al. Wnt activation and reduced cell–cell contact synergistically induce massive expansion of functional human iPSC-derived cardiomyocytes. *Cell Stem Cell* **27**, 50–63 (2020).
82. Guo, J. et al. Elastomer-grafted iPSC-derived micro heart muscles to investigate effects of mechanical loading on physiology. *ACS Biomater. Sci. Eng.* **7**, 2973–2989 (2021).
83. Dou, W. et al. A microdevice platform for characterizing the effect of mechanical strain magnitudes on the maturation of iPSC-cardiomyocytes. *Biosens. Bioelectron.* **175**, 112875 (2021).
84. Kroll, K. et al. Electro-mechanical conditioning of human iPSC-derived cardiomyocytes for translational research. *Prog. Biophys. Mol. Biol.* **130**, 212–222 (2017).
85. Noor, N. et al. 3D printing of personalized thick and perfusable cardiac patches and hearts. *Adv. Sci.* **6**, 1900344 (2019).
86. Schwan, J. et al. Anisotropic engineered heart tissue made from laser-cut decellularized myocardium. *Sci. Rep.* **6**, 32068 (2016).
87. Goldfracht, I. et al. Engineered heart tissue models from hiPSC-derived cardiomyocytes and cardiac ECM for disease modeling and drug testing applications. *Acta Biomater.* **92**, 145–159 (2019).
88. Blazeski, A. et al. Functional properties of engineered heart slices incorporating human induced pluripotent stem cell-derived cardiomyocytes. *Stem Cell Reports* **12**, 982–995 (2019).
89. Vannozzi, L. et al. Self-folded hydrogel tubes for implantable muscular tissue scaffolds. *Macromol. Biosci.* **18**, e1700377 (2018).
90. Abecasis, B. et al. Unveiling the molecular crosstalk in a human induced pluripotent stem cell-derived cardiac model. *Biotechnol. Bioeng.* **116**, 1245–1252 (2019).
91. Floy, M. E. et al. Direct coculture of human pluripotent stem cell-derived cardiac progenitor cells with epicardial cells induces cardiomyocyte proliferation and reduces sarcomere organization. *J. Mol. Cell. Cardiol.* **162**, 144–157 (2022).
92. Peters, M. C. et al. Follistatin-like 1 promotes proliferation of matured human hypoxic iPSC-cardiomyocytes and is secreted by cardiac fibroblasts. *Mol. Ther. Methods Clin. Dev.* **25**, 3–16 (2022).
93. Hookway, T. A. et al. Phenotypic variation between stromal cells differentially impacts engineered cardiac tissue function. *Tissue Eng. Part A* **25**, 773–785 (2019).
94. Rupert, C. E., Kim, T. Y., Choi, B. R. & Coulombe, K. L. K. Human cardiac fibroblast number and activation state modulate electromechanical function of hiPSC-cardiomyocytes in engineered myocardium. *Stem Cells Int.* **2020**, 9363809 (2020).
95. Giacomelli, E. et al. Human-iPSC-derived cardiac stromal cells enhance maturation in 3D cardiac microtissues and reveal non-cardiomyocyte contributions to heart disease. *Cell Stem Cell* **26**, 862–879 (2020).
An informative study parsing the impact of co-culture with cardiac fibroblasts and ECs on the maturation of hiPSC-CMs in scaffold-free cardiac spheroids.
96. Ahrens, J. H. et al. Programming cellular alignment in engineered cardiac tissue via bioprinting anisotropic organ building blocks. *Adv. Mater.* **34**, e2200217 (2022).
97. Feric, N. T. et al. Engineered cardiac tissues generated in the Biowire II: a platform for human-based drug discovery. *Toxicol. Sci.* **172**, 89–97 (2019).
98. Tamargo, M. A. et al. MilliPillar: a platform for the generation and real-time assessment of human engineered cardiac tissues. *ACS Biomater. Sci. Eng.* **7**, 5215–5229 (2021).
99. Ulmer, B. M. et al. Contractile work contributes to maturation of energy metabolism in hiPSC-derived cardiomyocytes. *Stem Cell Reports* **10**, 834–847 (2018).
100. Boudou, T. et al. A microfabricated platform to measure and manipulate the mechanics of engineered cardiac microtissues. *Tissue Eng. Part A* **18**, 910–919 (2012).
101. Lee, S. et al. Contractile force generation by 3D hiPSC-derived cardiac tissues is enhanced by rapid establishment of cellular interconnection in matrix with muscle-mimicking stiffness. *Biomaterials* **131**, 111–120 (2017).
102. Feaster, T. K. et al. A method for the generation of single contracting human-induced pluripotent stem cell-derived cardiomyocytes. *Circ. Res.* **117**, 995–1000 (2015).
103. Jayne, R. K. et al. Direct laser writing for cardiac tissue engineering: a microfluidic heart on a chip with integrated transducers. *Lab Chip* **21**, 1724–1737 (2021).
104. Rogers, A. J., Fast, V. G. & Sethu, P. Biomimetic cardiac tissue model enables the adaption of human induced pluripotent stem cell cardiomyocytes to physiological hemodynamic loads. *Anal. Chem.* **88**, 9862–9868 (2016).
105. Ng, R. et al. Contractile work directly modulates mitochondrial protein levels in human engineered heart tissues. *Am. J. Physiol. Heart Circ. Physiol.* **318**, 1516–1524 (2020).
106. Ma, X. et al. 3D printed micro-scale force gauge arrays to improve human cardiac tissue maturation and enable high throughput drug testing. *Acta Biomater.* **95**, 319–327 (2019).
107. Ruan, J. L. et al. Mechanical stress promotes maturation of human myocardium from pluripotent stem cell-derived progenitors. *Stem Cells* **33**, 2148–2157 (2015).
108. Kolanowski, T. J. et al. Enhanced structural maturation of human induced pluripotent stem cell-derived cardiomyocytes under a controlled microenvironment in a microfluidic system. *Acta Biomater.* **102**, 273–286 (2020).
109. Marsano, A. et al. Beating heart on a chip: a novel microfluidic platform to generate functional 3D cardiac microtissues. *Lab Chip* **16**, 599–610 (2016).

110. Gao, L. et al. Large cardiac muscle patches engineered from human induced-pluripotent stem cell-derived cardiac cells improve recovery from myocardial infarction in swine. *Circulation* **137**, 1712–1730 (2018).
111. Ribeiro, A. J. S. et al. Contractility of single cardiomyocytes differentiated from pluripotent stem cells depends on physiological shape and substrate stiffness. *Proc. Natl Acad. Sci. USA* **112**, 12705–12710 (2015).
112. Abilez, O. J. et al. Passive stretch induces structural and functional maturation of engineered heart muscle as predicted by computational modeling. *Stem Cells* **36**, 265–277 (2018).
113. Leonard, A. et al. Afterload promotes maturation of human induced pluripotent stem cell derived cardiomyocytes in engineered heart tissues. *J. Mol. Cell. Cardiol.* **118**, 147–158 (2018).
114. Bliley, J. M. et al. Dynamic loading of human engineered heart tissue enhances contractile function and drives a desmosome-linked disease phenotype. *Sci. Transl. Med.* **13**, 1817 (2021).
115. Ruan, J. L. et al. Mechanical stress conditioning and electrical stimulation promote contractility and force maturation of induced pluripotent stem cell-derived human cardiac tissue. *Circulation* **134**, 1557–1567 (2016).
116. Ronaldson-Bouchard, K. et al. Advanced maturation of human cardiac tissue grown from pluripotent stem cells. *Nature* **556**, 239–243 (2018).
- An informative study demonstrating the effectiveness of electromechanical training for the maturation of hiPSC-CMs.**
117. Yoshida, S. et al. Maturation of human induced pluripotent stem cell-derived cardiomyocytes by soluble factors from human mesenchymal stem cells. *Mol. Ther.* **26**, 2681–2695 (2018).
118. Yang, X. et al. Tri-iodo-L-thyronine promotes the maturation of human cardiomyocytes-derived from induced pluripotent stem cells. *J. Mol. Cell. Cardiol.* **72**, 296–304 (2014).
119. Correia, C. et al. Distinct carbon sources affect structural and functional maturation of cardiomyocytes derived from human pluripotent stem cells. *Sci. Rep.* **7**, 8590 (2017).
- An informative study demonstrating the link between metabolic substrate utilization and functional maturation of hiPSC-CMs.**
120. Zhao, B., Zhang, K., Chen, C. S. & Lejeune, E. Sarc-Graph: automated segmentation, tracking, and analysis of sarcomeres in hiPSC-derived cardiomyocytes. *PLoS Comput. Biol.* **17**, e1009443 (2021).
121. Toepfer, C. N. et al. SarcTrack. *Circ. Res.* **124**, 1172–1183 (2019).
122. Morrill, E. E. et al. A validated software application to measure fiber organization in soft tissue. *Biomech. Model. Mechanobiol.* **15**, 1467–1478 (2016).
123. Stein, J. M. et al. Software tool for automatic quantification of sarcomere length and organization in fixed and live 2D and 3D muscle cell cultures in vitro. *Curr. Protoc.* **2**, e462 (2022).
124. Sutcliffe, M. D. et al. High content analysis identifies unique morphological features of reprogrammed cardiomyocytes. *Sci. Rep.* **8**, 1258 (2018).
125. Mills, R. J. et al. Functional screening in human cardiac organoids reveals a metabolic mechanism for cardiomyocyte cell cycle arrest. *Proc. Natl Acad. Sci. USA* **114**, E8372–E8381 (2017).
126. Fukushima, H. et al. Specific induction and long-term maintenance of high purity ventricular cardiomyocytes from human induced pluripotent stem cells. *PLoS ONE* **15**, e0241287 (2020).
127. Garay, B. I. et al. Dual inhibition of MAPK and PI3K/AKT pathways enhances maturation of human iPSC-derived cardiomyocytes. *Stem Cell Reports* **17**, 2005–2022 (2022).
128. Ergir, E. et al. Generation and maturation of human iPSC-derived 3D organotypic cardiac microtissues in long-term culture. *Sci. Rep.* **12**, 17409 (2022).
129. Cui, N. et al. Doxorubicin-induced cardiotoxicity is maturation dependent due to the shift from topoisomerase II α to II β in human stem cell derived cardiomyocytes. *J. Cell. Mol. Med.* **23**, 4627–4639 (2019).
130. Jabbour, R. J. et al. In vivo grafting of large engineered heart tissue patches for cardiac repair. *JCI Insight* **6**, e144068 (2021).
131. Hatani, T. et al. Nano-structural analysis of engrafted human induced pluripotent stem cell-derived cardiomyocytes in mouse hearts using a genetic-probe APEX2. *Biochem. Biophys. Res. Commun.* **505**, 1251–1256 (2018).
132. Kerscher, P. et al. Direct hydrogel encapsulation of pluripotent stem cells enables ontomimetic differentiation and growth of engineered human heart tissues. *Biomaterials* **83**, 383–395 (2016).
133. Huang, C. Y. et al. Enhancement of human iPSC-derived cardiomyocyte maturation by chemical conditioning in a 3D environment. *J. Mol. Cell. Cardiol.* **138**, 1–11 (2020).
134. Mannhardt, I. et al. Human engineered heart tissue: analysis of contractile force. *Stem Cell Reports* **7**, 29–42 (2016).
135. Shadrin, I. Y. et al. Cardiopatch platform enables maturation and scale-up of human pluripotent stem cell-derived engineered heart tissues. *Nat. Commun.* **8**, 1825 (2017).
136. Huebsch, N. et al. Automated video-based analysis of contractility and calcium flux in human-induced pluripotent stem cell-derived cardiomyocytes cultured over different spatial scales. *Tissue Eng. Part C Methods* **21**, 467–479 (2015).
137. Sharma, A., Toepfer, C. N., Schmid, M., Garfinkel, A. C. & Seidman, C. E. Differentiation and contractile analysis of GFP-sarcomere reporter hiPSC-cardiomyocytes. *Curr. Protoc. Hum. Genet.* **96**, 21.12.1–21.12.12 (2018).
138. Maddah, M. et al. A non-invasive platform for functional characterization of stem-cell-derived cardiomyocytes with applications in cardiotoxicity testing. *Stem Cell Reports* **4**, 621–631 (2015).
139. Psaras, Y. et al. CalTrack: high-throughput automated calcium transient analysis in cardiomyocytes. *Circ. Res.* **129**, 326–341 (2021).
140. Yang, H. et al. Deriving waveform parameters from calcium transients in human iPSC-derived cardiomyocytes to predict cardiac activity with machine learning. *Stem Cell Reports* **17**, 556–568 (2022).
141. Shroff, S. N. et al. Voltage imaging of cardiac cells and tissue using the genetically encoded voltage sensor archon1. *iScience* **23**, 100974 (2020).
142. Lopaschuk, G. D., Spafford, M. A. & Marsh Cardiovascular, D. R. Glycolysis is predominant source of myocardial ATP production immediately after birth. *Am. J. Physiol.* **216**, 1698–1705 (1991).
143. Murashige, D. et al. Comprehensive quantification of fuel use by the failing and nonfailing human heart. *Science* **370**, 364–368 (2020).
144. Bhute, V. J. et al. Metabolomics identifies metabolic markers of maturation in human pluripotent stem cell-derived cardiomyocytes. *Theranostics* **7**, 2078–2091 (2017).
145. Yang, X. et al. Fatty acids enhance the maturation of cardiomyocytes derived from human pluripotent stem cells. *Stem Cell Reports* **13**, 657–668 (2019).
146. Horikoshi, Y. et al. Fatty acid-treated induced pluripotent stem cell-derived human cardiomyocytes exhibit adult cardiomyocyte-like energy metabolism phenotypes. *Cells* **8**, 1095 (2019).
147. Zhang, J. Z. et al. A human iPSC double-reporter system enables purification of cardiac lineage subpopulations with distinct function and drug response profiles. *Cell Stem Cell* **24**, 802–811 (2019).
148. Da Rocha, A. M. et al. hiPSC-CM monolayer maturation state determines drug responsiveness in high throughput pro-arrhythmia screen. *Sci. Rep.* **7**, 13834 (2017).

149. Huebsch, N. et al. Metabolically driven maturation of human-induced-pluripotent-stem-cell-derived cardiac microtissues on microfluidic chips. *Nat. Biomed. Eng.* **6**, 372–388 (2022).
An informative study using microfluidic chips and metabolic maturation to improve the alignment and maturation of hiPSC-CMs.
150. Lemcke, H., Skorska, A., Lang, C. I., Johann, L. & David, R. Quantitative evaluation of the sarcomere network of human hiPSC-derived cardiomyocytes using single-molecule localization microscopy. *Int. J. Mol. Sci.* **21**, 2819 (2020).
151. Yang, B. et al. A net mold-based method of biomaterial-free three-dimensional cardiac tissue creation. *Tissue Eng. Part C Methods* **25**, 243–252 (2019).
152. Piccini, I., Rao, J., Seeböhm, G. & Greber, B. Human pluripotent stem cell-derived cardiomyocytes: genome-wide expression profiling of long-term in vitro maturation in comparison to human heart tissue. *Genom. Data* **4**, 69–72 (2015).
153. Tsui, J. H. et al. Tunable electroconductive decellularized extracellular matrix hydrogels for engineering human cardiac microphysiological systems. *Biomaterials* **272**, 120764 (2021).
154. Guyette, J. P. et al. Bioengineering human myocardium on native extracellular matrix. *Circ. Res.* **118**, 56–72 (2016).
155. Zhao, Y. et al. A platform for generation of chamber-specific cardiac tissues and disease modeling. *Cell* **176**, 913–927 (2019).
156. Pretorius, D. et al. Layer-by-layer fabrication of large and thick human cardiac muscle patch constructs with superior electrophysiological properties. *Front. Cell Dev. Biol.* **9**, 670504 (2021).
157. Geng, L. et al. Rapid electrical stimulation increased cardiac apoptosis through disturbance of calcium homeostasis and mitochondrial dysfunction in human induced pluripotent stem cell-derived cardiomyocytes. *Cell. Physiol. Biochem.* **47**, 1167–1180 (2018).
158. Dickerson, D. A. Advancing engineered heart muscle tissue complexity with hydrogel composites. *Adv. Biol.* **7**, e2200067 (2023).
159. Tani, H. et al. Heart-derived collagen promotes maturation of engineered heart tissue. *Biomaterials* **299**, 122174 (2023).
160. Kaiser, N. J., Kant, R. J., Minor, A. J. & Coulombe, K. L. K. Optimizing blended collagen–fibrin hydrogels for cardiac tissue engineering with human iPSC-derived cardiomyocytes. *ACS Biomater. Sci. Eng.* **5**, 887–899 (2019).
161. Lv, W., Babu, A., Morley, M. P., Musunuru, K. & Guerraty, M. Resource of gene expression data from a multiethnic population cohort of induced pluripotent cell-derived cardiomyocytes. *Circ. Genom. Precis. Med.* **17**, e004218 (2024).
162. Soepriatna, A. H. et al. Action potential metrics and automated data analysis pipeline for cardiotoxicity testing using optically mapped hiPSC-derived 3D cardiac microtissues. *PLoS ONE* **18**, e0280406 (2023).
163. Olivetti, G. et al. Aging, cardiac hypertrophy and ischemic cardiomyopathy do not affect the proportion of mononucleated and multinucleated myocytes in the human heart. *J. Mol. Cell. Cardiol.* **28**, 1463–1477 (1996).
164. Squire, J. M. Architecture and function in the muscle sarcomere. *Curr. Opin. Struct. Biol.* **7**, 247–257 (1997).
165. Martin Gerdes, A. et al. Structural remodeling of cardiac myocytes in patients with ischemic cardiomyopathy. *Circulation* **86**, 426–430 (1992).
166. Feric, N. T. & Radisic, M. Maturing human pluripotent stem cell-derived cardiomyocytes in human engineered cardiac tissues. *Adv. Drug Deliv. Rev.* **96**, 110–134 (2016).
167. Porter, G. A. et al. Bioenergetics, mitochondria, and cardiac myocyte differentiation. *Prog. Pediatr. Cardiol.* **31**, 75–81 (2011).
168. Nagueh, S. F. et al. Altered titin expression, myocardial stiffness, and left ventricular function in patients with dilated cardiomyopathy. *Circulation* **110**, 155–162 (2004).
169. Van Der Velden, J. et al. Isometric tension development and its calcium sensitivity in skinned myocyte-sized preparations from different regions of the human heart. *Cardiovasc. Res.* **42**, 706–719 (1999).
170. Hasenfuss, G. et al. Energetics of isometric force development in control and volume-overload human myocardium comparison with animal species. *Circ. Res.* **68**, 836–846 (1990).
171. Tenreiro, M. F., Louro, A. F., Alves, P. M. & Serra, M. Next generation of heart regenerative therapies: progress and promise of cardiac tissue engineering. *NPJ Regen. Med.* **6**, 30 (2021).
172. Drouin, E., Charpentier, F., Gauthier, C., Laurent, K. & Le Marec, H. Electrophysiologic characteristics of cells spanning the left ventricular wall of human heart: evidence for presence of M cells. *J. Am. Coll. Cardiol.* **26**, 185–192 (1995).
173. Koncz, I. et al. Electrophysiological effects of ivabradine in dog and human cardiac preparations: potential antiarrhythmic actions. *Eur. J. Pharmacol.* **668**, 419–426 (2011).
174. Dangman, K. H. et al. Electrophysiologic characteristics of human ventricular and Purkinje fibers. *Circulation* **65**, 362–368 (1982).
175. Carafoli, E., Santella, L., Branca, D. & Brini, M. Generation, control, and processing of cellular calcium signals. *Crit. Rev. Biochem. Mol. Biol.* **36**, 107–260 (2001).

Acknowledgements

This work was funded by the National Science Foundation (NSF) Engineering Research Center on Cellular Metamaterials (EEC-1647837). J.K.E. acknowledges financial support from the National Institutes of Health National Heart, Lung, and Blood Institute (F31 HL158195). S.J.D. and B.M.B. acknowledge financial support from the NSF (2033654). S.J.D. acknowledges support from the National Institutes of Health (T32-DE007057 and T32-HL125242). J.K.E. and X.G. acknowledge funding support from the NSF Graduate Research Fellowship Program. L.L. acknowledges support provided by the Florida Heart Research Foundation. C.S.C. acknowledges support from the NSF (CMMI-1548571 and DGE-2244366) and the Paul G. Allen Frontiers Group Allen Distinguished Investigator Program.

Author contributions

J.K.E. and S.J.D. contributed equally, led and performed analysis, and wrote and reviewed the manuscript. B.M.B. and C.S.C. jointly supervised this work and wrote and reviewed the manuscript. M.E.J., M.Ç.K., Y.-M.L., P.M.H., X.G., L.L., M. McLellan, J.T., M. Ma and A.C.S.C. performed analysis and reviewed the manuscript. J.H., K.C.T., T.G.B., S.R., A.E.W., A.A. and E.L. supervised analysis and reviewed the manuscript.

Competing interests

C.S.C. is a founder and owns shares of Satellite Biosciences, a company that is developing cell-based therapies; and Ropirio Therapeutics, a company that is developing pharmaceuticals. All other authors declare no competing interests.

Additional information

Supplementary information The online version contains supplementary material available at <https://doi.org/10.1038/s41592-024-02480-7>.

Correspondence should be addressed to Brendon M. Baker or Christopher S. Chen.

Peer review information *Nature Methods* thanks Nathan Palpant and the other, anonymous, reviewer(s) for their contribution to the peer review of this work. Primary Handling Editor: Madhura Mukhopadhyay, in collaboration with the *Nature Methods* team.

Reprints and permissions information is available at www.nature.com/reprints.

Publisher's note Springer Nature remains neutral with regard to jurisdictional claims in published maps and institutional affiliations.

Springer Nature or its licensor (e.g. a society or other partner) holds exclusive rights to this article under a publishing agreement with

the author(s) or other rightsholder(s); author self-archiving of the accepted manuscript version of this article is solely governed by the terms of such publishing agreement and applicable law.

© Springer Nature America, Inc. 2024

¹Department of Biomedical Engineering, Boston University, Boston, MA, USA. ²Department of Biomedical Engineering, University of Michigan, Ann Arbor, MI, USA. ³Department of Mechanical Engineering, Boston University, Boston, MA, USA. ⁴Photonics Center, Boston University, Boston, MA, USA. ⁵Department of Biomedical Engineering, Florida International University, Miami, FL, USA. ⁶Harvard–MIT Program in Health Sciences and Technology, Institute for Medical Engineering and Science, Massachusetts Institute of Technology, Cambridge, MA, USA. ⁷Wyss Institute for Biologically Inspired Engineering, Harvard University, Boston, MA, USA. ⁸Department of Mechanical and Material Engineering, Florida International University, Miami, FL, USA. ⁹Department of Physics, Florida International University, Miami, FL, USA. ¹⁰School of Engineering, Brown University, Providence, RI, USA. ¹¹Brown–Lifespan Center for Digital Health, Providence, RI, USA. ¹²Division of Materials Science and Engineering, Boston University, Boston, MA, USA. ¹³Department of Physics, Boston University, Boston, MA, USA. ¹⁴These authors contributed equally: Jourdan K. Ewoldt, Samuel J. DePalma. ✉e-mail: bambren@umich.edu; chencs@bu.edu